2002

Biomass reburning for control of nitrogen oxides

Jeffrey James Sweterlitsch
Iowa State University

INFORMATION TO USERS

This manuscript has been reproduced from the microfilm master. UMI films the text directly from the original or copy submitted. Thus, some thesis and dissertation copies are in typewriter face, while others may be from any type of computer printer.

The quality of this reproduction is dependent upon the quality of the copy submitted. Broken or indistinct print, colored or poor quality illustrations and photographs, print bleedthrough, substandard margins, and improper alignment can adversely affect reproduction.

In the unlikely event that the author did not send UMI a complete manuscript and there are missing pages, these will be noted. Also, if unauthorized copyright material had to be removed, a note will indicate the deletion.

Oversize materials (e.g., maps, drawings, charts) are reproduced by sectioning the original, beginning at the upper left-hand corner and continuing from left to right in equal sections with small overlaps.

ProQuest Information and Learning
300 North Zeeb Road, Ann Arbor, MI 48106-1346 USA
800-521-0600

Biomass reburning for control of nitrogen oxides

by

Jeffrey James Sweterlitsch

A dissertation submitted to the graduate faculty

in partial fulfillment of the requirements for the degree of

DOCTOR OF PHILOSOPHY

Major: Chemical Engineering

Program of Study Committee:
Robert C. Brown (Major Professor)
Francine Battaglia
Kenneth M. Bryden
Peter J. Reilly
Brent H. Shanks

Iowa State University

Ames, Iowa

2002

Graduate College
Iowa State University

This is to certify that the doctoral dissertation of

Jeffrey James Sweterlitsch

has met the dissertation requirements of Iowa State University

Signature was redacted for privacy.

Major Professor

Signature was redacted for privacy.

For the Major Program

TABLE OF CONTENTS

LIST OF FIGURES

LIST OF TABLES

ACKNOWLEDGEMENTS

Several people made this research possible. Professor Robert C. Brown served as my academic advisor, providing me with support and direction for this research. Professors Kenneth M. Bryden, Peter J. Reilly, Brent H. Shanks, and Francine Battaglia served on my committee.

Bernard Breen and Joseph Urich of Energy Systems Associates, Inc. provided technical assistance in devising the experimental program.

Jerod Smeenk, Andy Suby, Thomas Cauley, and Hongqun Yang provided technical assistance in the laboratory.

ABSTRACT

Fuel-Lean Gas Reburning™ (FLGR) is a method of controlling NO_x emissions produced during coal combustion in utility boilers by injecting natural gas into the boiler downstream of the primary combustion zone. Whereas traditional reburning requires 10% – 20% of the total energy input from the reburn fuel followed by over-fire air to complete combustion of fuel fragments, FLGR uses only 5% – 10% of the total energy input from the reburn fuel. Because less fuel is used, the overall environment in the boiler remains fuel-lean, with only localized eddies that are fuel-rich, where the NO_x reduction takes place. FLGR does not require over-fire air to complete the combustion of fuel fragments. Fuel-lean biomass reburning is a variation of FLGR that uses biomass instead of natural gas as the reburn fuel.

The goal of this work was to simulate a coal-fired utility boiler in an experimental down-flow reactor, and evaluate the influence of several variables, including the initial oxygen concentration, the type of biomass used, the % energy input from biomass, and the type of carrier gas used for injecting the biomass into the reactor.

CHAPTER 1. INTRODUCTION

The goal of this work was to simulate a coal-fired utility boiler in an experimental down-flow reactor to evaluate the effectiveness of biomass as a reburn fuel as a means to reduce nitrogen oxides emissions.

Nitrogen oxides are formed during the combustion of coal and contribute to the formation of smog and acid rain. In an effort to control these emissions, Congress passed the Clean Air Act Amendments of 1990, which set standards for many types of sources of pollution, including stationary coal-fired utility boilers. These Amendments include statements that encourage the development of new technologies that will meet these new emissions limits. Reburning is one of these technologies.

Reburning technology is a process that manipulates the chemistry associated with the combustion of fuel so as to limit the overall production of nitrogen oxides. To inhibit the formation of nitrogen oxides, combustion is staged within the reactor, promoting chemical reactions that would otherwise not occur, and creating a regime where molecular nitrogen (N_2), rather than the combustion products nitrogen oxides, are favored. A variety of different fuels can be used, not just the fuel that is used in the first stage of the combustion process. Natural gas is commonly used as a reburn fuel, but it is a non-renewable fuel source and the combustion of natural gas results in a net increase of carbon dioxide in the atmosphere. Biomass, whether wood, herbaceous crops, or agricultural residues, is a renewable fuel source. The carbon dioxide formed by burning biomass is offset by the carbon dioxide absorbed by the biomass during growth, so there is no net increase of carbon dioxide in the atmosphere.

Fuel-Lean Gas Reburning™ (FLGR), developed by Energy Systems Associates, Inc., is a method of controlling NO_x emissions produced during coal combustion in utility boilers by injecting natural gas into the boiler downstream of the primary combustion zone. Whereas traditional reburning requires 10% – 20% of the total energy input from the reburn fuel, followed by over-fire air to complete combustion of fuel fragments, FLGR uses only 5% – 10% of the total energy input from the reburn fuel. Because less fuel is used, the overall environment in the boiler remains fuel-lean, with only localized eddies that are fuel-rich where the NO_x reduction takes place. FLGR does not require over-fire air to complete the combustion of fuel fragments. Fuel-Lean Biomass Reburning is a variation of FLGR that uses biomass instead of natural gas as the reburn fuel. Figure 1 is a schematic of the FLGR process.

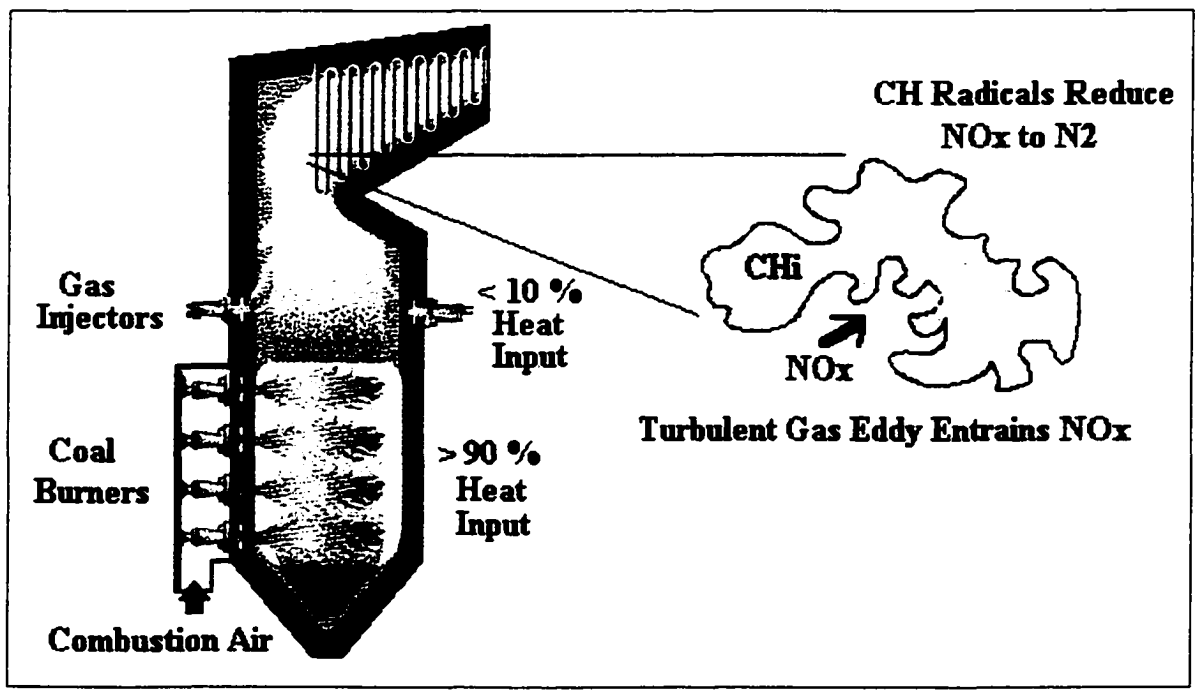

Figure 1. Schematic of the Fuel-Lean Gas Reburn Process

Pulverized coal boilers and stoker boilers were simulated by varying the amount of air that was reacted: lower flow rates of air, producing initial O_2 concentrations of 1% – 4%, represented pulverized coal boilers, while higher flow rates of air, producing initial O_2 concentrations of 5% – 6%, represented stoker boilers. Stoker boilers typically have shorter residence times and lower operating temperatures, and increasing the air flow rate produces both conditions simultaneously within the experimental down-flow reactor [1]. The primary fuel for the down-flow reactor was not coal, but natural gas. Tracer gas experiments and computational fluid dynamics modeling was used to study the mixing characteristics of the flue gas and the injected biomass.

Two types of biomass, low nitrogen-containing switchgrass and high nitrogen-containing alfalfa, were used. By comparing a high nitrogen-containing biomass fuel with a low nitrogen-containing biomass fuel, it could be determined if there was any amine-enhancement during the reburning process [2]. Injecting the biomass into the down-flow reactor was done pneumatically, using nitrogen and/or steam. By using steam it is proposed that the biomass would gasify in situ, generating more volatiles to react with the NO_x.

CHAPTER 2. BACKGROUND

2.1. The Clean Air Act Amendments of 1990

The Air Pollution Control Act of 1955 was the first of several acts and amendments that the federal government passed to tackle the growing problem of air pollution. Over the next thirty-five years, Congress passed several amendments and acts related to air pollution, with each act or amendment designating increased amounts of funding for research in air pollution formation and control. The amendments also helped to establish emission standards for both vehicular sources and stationary sources [3]. With the Clean Air Act Amendments of 1990, the federal government addressed five main areas: air-quality standards, motor vehicle emissions and alternative fuels, toxic air pollutants, acid rain, and stratospheric ozone depletion [3].

Title I of the Clean Air Act Amendments of 1990 (CAAA) required Reasonably Available Control Technology (RACT) to be adopted by major NO_x sources [4], as Congress had determined,

> . . . that the predominant part of the Nation's population is located in its rapidly expanding metropolitan and other urban areas, . . . [and] the growth in . . . air pollution brought about by urbanization, industrial development, and the increasing use of motor vehicles, has resulted in mounting dangers to the public health and welfare , . . . that air pollution prevention [and] . . . control at its source is the primary responsibility of the States and local governments; and that Federal financial assistance and leadership is essential for the development of . . . programs to prevent and control air pollution [5].

NO_x emissions impacts public health and the environment in several ways, including acid deposition, high levels of nitrates in drinking water, eutrophication (accelerated algae and aquatic plant growth), global warming, nitrate particle and acid aerosols formations, and stratospheric ozone depletion [6].

Title IV of the CAAA ". . . created a two-phased plan . . . to reduce acid rain in the United States. Phase I runs from 1995 through 1999, and Phase II . . . begins in 2000." [7]. Over 400 units are affected by Phase I, and over 2000 units will be affected by Phase II. Different emission limitations were applied to different types of boilers. According to the CAAA, the maximum emission rates for a tangentially fired boiler is 0.45 lb/MMBTU and for a dry bottom wall-fired boiler is 0.50 lb/MMBTU [7]. A "dry bottom wall-fired" boiler operates at a low enough temperature so that the ash remains in solid form, and the burners are oriented perpendicular to the walls of the combustion chamber; "wet-fired" refers to a boiler that operates at a high enough temperature so that it melts the ash; and "tangentially-fired" refers to an orientation of the burners within the chamber so that a swirling flame is produced [7,8]. In a cyclone boiler, "[c]ombustion occurs within water-cooled horizontal cylinders, called cyclones, attached to the sides of the boiler . . . designed to create high-turbulence, high-temperature . . . conditions sufficient to transform coal ash to molten slag, thereby reducing the fly ash content of the flue gas."[9] Tangentially-fired and wall-fired boilers use pulverized coal, while cyclone boilers use crushed coal, which is cheaper to process.

2.2. Formation of Nitrogen Oxides

Nitrogen oxides, which are comprised of nitric oxide (NO), nitrous oxide (N_2O), and nitrogen dioxide (NO_2), and are often referred to as a collective NO_x, are formed during the combustion of fuels in three ways. The first method, thermally formed NO_x, is described by the Zeldovich mechanism:

$$O + N_2 \longleftrightarrow NO + N, \tag{1}$$

$$N + O_2 \longleftrightarrow NO + O. \tag{2}$$

The rate constants for the reactions are [10]:

$$k_1 = 1.36 \cdot 10^{14} \cdot \exp\frac{-75.4\ kcal}{RT} \quad \text{cm}^3/\text{mol sec}, \tag{3}$$

$$k_2 = 6.4 \cdot 10^{9} \cdot T \cdot \exp\frac{-6.25\ kcal}{RT} \quad \text{cm}^3/\text{mol sec}, \tag{4}$$

$$k_{-2} = 1.55 \cdot 10^{9} \cdot T \cdot \exp\frac{-38.6\ kcal}{RT} \quad \text{cm}^3/\text{mol sec}. \tag{5}$$

In a high temperature environment, the formation of NO will be fast in the presence of O atoms. The concentration of NO will not decrease appreciably as the gases cool because the reverse reaction, k_{-2}, is more temperature dependent due to a larger activation energy [10]. Thermally formed NO_x is commonly thought to be formed from air that is heated in the presence of the combustion flame, and not from nitrogen that may be present in the fuel [11].

The second method of NO_x formation is due to fuel-bound nitrogen (FBN). In a fuel-rich section of the combustion flame, FBN reacts to form NH_3 and HCN, which are oxidized to form NO_x in the fuel-lean section of the combustion flame. If these intermediate species are exposed to high temperatures and a reducing environment (fuel-rich) for a significant length of time, they can be converted into molecular nitrogen (N_2), rather than NO_x. The third way is prompt NO_x, where fuel fragments, such as CH_i, form to react with atmospheric nitrogen to form amino and cyano species comparable to those described previously. These species are then oxidized to form NO_x [12].

2.3. Methods of Reducing NO_x Emissions

There are several ways to reduce the formation and emission of NO_x. Each method involves a process in which the temperature of the flame is reduced and the reaction time is

increased. These processes include air staging, flue gas recirculation, operating with low excess air, selective catalytic and non-catalytic means, and fuel staging or reburning, which is the method employed in this research.

Air staging is a process where the combustion air is fed to the process stream in two locations, creating a fuel-rich primary zone and a fuel-lean secondary zone. The primary zone lacks sufficient oxygen for FBN-formed NO_x, so the nitrogen that is released during combustion forms molecular nitrogen. The secondary zone operates under fuel-lean conditions, which would normally promote thermal NO_x, but the temperature is significantly lower because heat is removed following the primary zone. Air-staged burners are usually applied to solid and liquid fuels [12,13].

Flue gas recirculation is a process where part of the hot flue gas is recirculated and mixed with the combustion air. This process acts as a diluent, reducing the temperature of the flame and reducing the concentration of oxygen available for both thermal NO_x and FBN NO_x formation. Flue gas recirculation is best suited for gas burners [12,13]. Using low excess air [13,14] is another way to reduce the formation of thermal NO_x, but operating at near stoichiometric conditions results in incomplete combustion, leading to carbon build-up and an unstable flame [14].

Two additional methods employed by industry to reduce NO_x emissions are selective non-catalytic reduction (SNCR) and selective catalytic reduction (SCR). Selective non-catalytic reduction involves the injection of a particular chemical species, such as ammonia or urea, into the process stream, converting NO_x to nitrogen. Selective catalytic reduction, as the name implies, converts NO_x to nitrogen using catalysts. SCR is commonly used today.

2.4. Reburning Technology

Reburning technology was developed by Wendt et al. [14] to reduce sulfur trioxide (SO_3) and NO_x emissions formed during the combustion of fossil fuels. As described by Wendt:

> The SO_3 can form sulfuric acid plumes and cause corrosion in the low-temperature zones of the furnace and, hence, can limit the combustion of sulfur-bearing fuels, even when regulations on sulfur dioxide are met," and "nitrogen oxides, from the combustion of fuels containing chemically bound nitrogen, contribute substantially to air pollution in the United States [14].

The reburning process for the combustion of fuel consists of three different theoretical regions within the combustion chamber. Combustion of the main source of fuel takes place in the primary zone, which is operated with excess air to insure more complete combustion. Within this zone the majority of FBN-NO_x and thermal-NO_x is formed. The second zone, called the reburning zone, involves the injection of a secondary fuel, called reburning fuel, to create a fuel-rich environment. Within this fuel-rich environment, some of the NO_x that formed in the primary zone, as well as some of FBN that may present in the reburning fuel, is chemically reduced to molecular nitrogen. In the third zone, called the burnout zone, air is added to complete the combustion of any fuel fragments not previously consumed [4,8,9,14-21].

Several researchers have examined reburning conditions that optimize NO_x reduction. These important variables include temperature, type of reburning fuel, primary and reburning air/fuel ratios, the reburning fuel/primary fuel ratio, and the residence time for the different stages. The temperature of the reburning zone, that is, the temperature at which the reburning fuel is injected into the process stream, was determined to be best suited at high temperatures, between 1570 K and around 1833 K, and the burnout temperature, or the

temperature at which the overfire air is injected, was lower, between 1200 K and 1450 K [9,16,17,19-21]. A wide variety of reburning fuels were considered, including fossil fuels such as coal and natural gas [14-16,22], and several renewable fuel sources, such as tire-derived fuel and wood [19,21,23,24]. The researchers concluded that reburning fuels high in volatiles and low in nitrogen are preferred [9,19,21,22].

2.5. Chemistry of Reburning

The chemistry of the reburning process takes place in the fuel-rich reburning zone, where several free radical reactions occur. Kilpinen et al. [17] identified and modeled 225 reversible, elementary gas-phase reactions involving 48 chemical species to describe this process. Bilbao et al. [25] developed a simplified model consisting of 87 reversible, elementary gas-phase reaction involving 38 chemical species. The general scheme comprises a multi-step process to convert NO_x to N_2 by the action of hydrocarbon radicals. The process begins with the formation of CH radicals and other hydrocarbon fuel fragments from the reburning fuel. More volatile reburning fuels produce more fuel fragments. CH radicals react with NO to form primarily HCN:

$$CH_i + NO \rightarrow HCN + products, \quad i = 1, 2. \tag{6}$$

Reaction of HCN with other free radicals produces additional nitrogenous species:

$$HCN + (H, O, OH) \rightarrow NH_i + products. \tag{7}$$

These nitrogenous species react further with NO to produce diatomic nitrogen:

$$NH_i + NO \rightarrow N_2 + products, \quad i = 0, 1, 2. \tag{8}$$

Other important chemical species in the reburning environment include ammonia produced by the partial equilibrium of the reaction

$$NH_i + OH \rightarrow NH_{i-1} + H_2O, \quad i = 1, 2, 3 \tag{9}$$

and nitrous oxide produced by the reaction

$$NH + NO \rightarrow N_2O + H \tag{10}$$

which can also be reduced to N_2 by

$$N_2O + H \rightarrow N_2 + OH. \tag{11}$$

2.6. Fuel-Lean Gas Reburning™

Fuel-Lean Gas Reburning™ (FLGR) was developed by Energy Systems Associates, Inc., and varies from traditional reburning in that there are only two stages, the primary zone and the reburning zone. Traditional reburning designates 10 – 20% of the total thermal output to come from the reburn fuel, while FLGR only uses 5 – 10% of the total thermal output, and is able to maintain overall fuel-lean conditions without the need of any additional air to complete the combustion of any fuel fragments not previously consumed in the reburn zone. FLGR is able to achieve reductions of 30 – 40% at a much lower capital investment than traditional reburning because there is less retrofitting required to employ FLGR. High velocity jets of natural gas are injected downstream of the main combustion zone in order to target certain areas within the boiler, creating locally fuel-rich eddies where NO_x is reduced to nitrogen. When biomass is used as the reburn fuel, the process is called Fuel-Lean Biomass Reburn (FLBR).

CHAPTER 3. EXPERIMENTAL METHODS AND PROCEDURES

The experiments performed in this research simulates the reburning process that occurs within turbulent eddies; they do not account for the mixing that would occur downstream of fuel-rich and fuel-lean eddies. As explained previously, Fuel-Lean Reburning uses only 5% – 10 % of the total energy input, averaged across the entire boiler volume. Within some turbulent eddies, however, the % energy input for a given volume of flue gas can and does exceed 10% energy input. The small scale of the down-flow reactor was not capable of simulating a full-scale boiler because in a full-scale boiler there would be significant radial species concentration gradients, temperature gradients, and a much higher degree of turbulence. Many of the experiments performed in the laboratory use more than 10% energy input from biomass as the reburn fuel.

Pulverized coal boilers and stoker boilers were simulated by varying the amount of air that was reacted: lower flow rates of air, producing initial O_2 concentrations of 1%, 2%, 3%, and 4%, represented pulverized coal boilers, while higher flow rates of air, producing initial O_2 concentrations of 5% and 6%, represented stoker boilers. The primary fuel for the down-flow reactor was not coal, but natural gas. Natural gas combustion does not produce as much nitrogen oxides as coal combustion, so a small amount of anhydrous ammonia (0.45% by volume of the total gaseous fuel input) was introduced into the natural gas line to artificially increase the initial NO_x concentrations, approaching those of coal combustion.

Two types of biomass, low nitrogen-containing switchgrass and high nitrogen-containing alfalfa, were used. Injecting the biomass into the down-flow reactor was done pneumatically, using nitrogen and/or steam. By using steam it is proposed that the biomass would gasify in situ, generating more volatiles to react with the NO_x.

3.1. Experimental Apparatus

The down-flow reactor consists of a natural gas burner, an insulated reaction chamber where the reburning process occurs, and a flue gas exhaust system. Figure 2 is a schematic of the experimental apparatus.

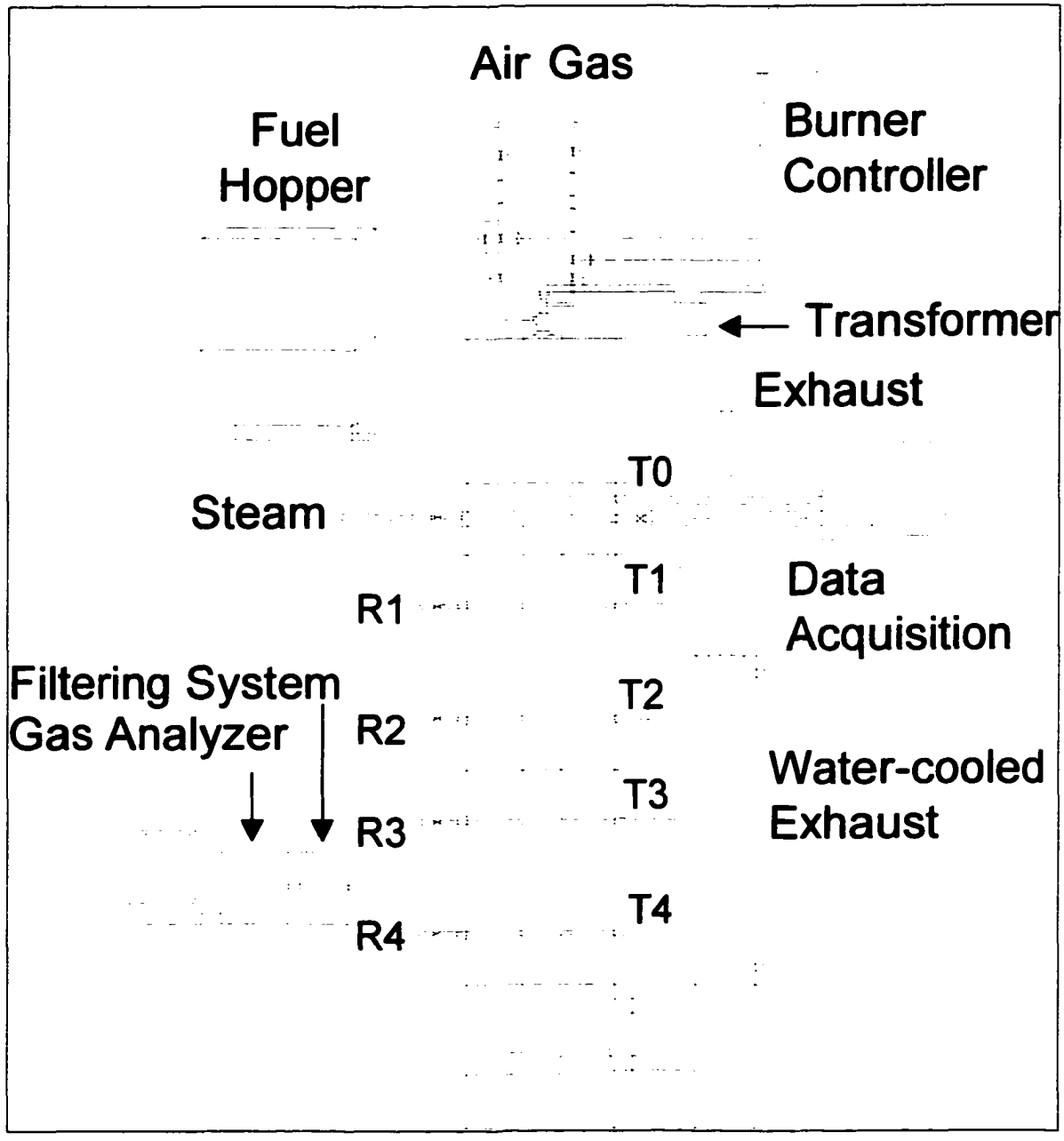

Figure 2. Schematic of Experimental Apparatus.

The natural gas burner is a Kromschroder, Inc., BIC50 nozzle-mixed burner nominally rated at 35 kW. The burner consists of a cast-iron housing, a stainless steel burner manifold where the air and natural gas mix, and a 0.31 m (12 in) long silicon carbide burner tube, which completes the combustion of the natural gas. Figure 3 shows the burner mounted on top of the reactor. The insulated reaction chamber consists of seven separate reactor sections that can be arranged in several configurations. Each section consists of a 0.15 m (6 in) diameter opening insulated by 0.23 m (9 in) thick castable ceramic, enclosed by a 9.5 mm (0.38 in) thick steel shell. Figure 4 shows the configuration employed in this current research. Also shown in Figure 4 is the biomass hopper and the water jacket to cool the exhaust.

Figure 5 is of the main control panel. On this control panel the primary air and natural gas flow rates are controlled with rotameters and measured with digital flow meters. Also controlled on this panel are the water flow rate for the water jacket, the carrier gas flow rate for biomass injection, and the ammonia flow rate, which is used for doping the natural gas with ammonia to produce NO_x emissions. The large enclosure shown on the right of this photograph contains the automatic controller for the natural gas burner. There is also a power switch to turn on/off the biomass hopper. A dial located next to the biomass hopper sets the flow rate of biomass.

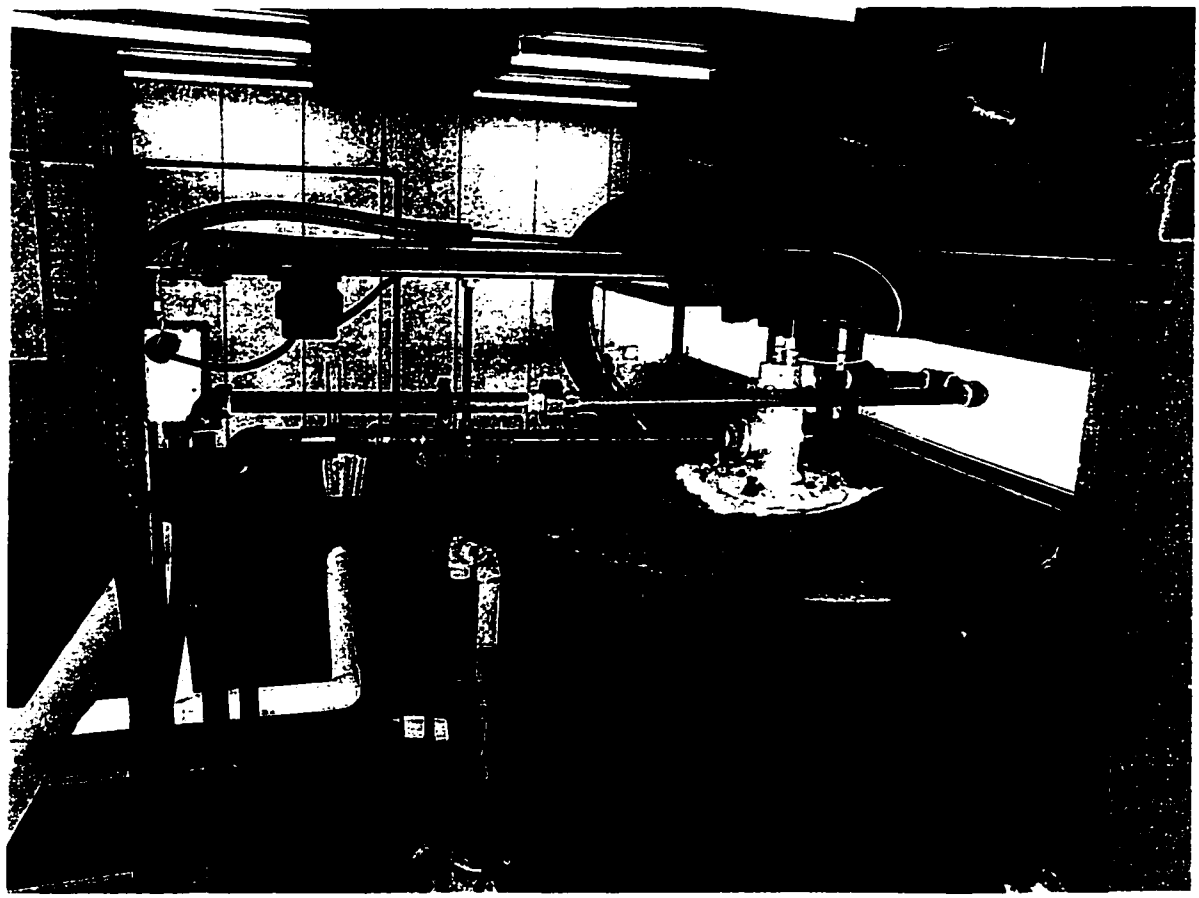

Figure 3. Natural gas burner.

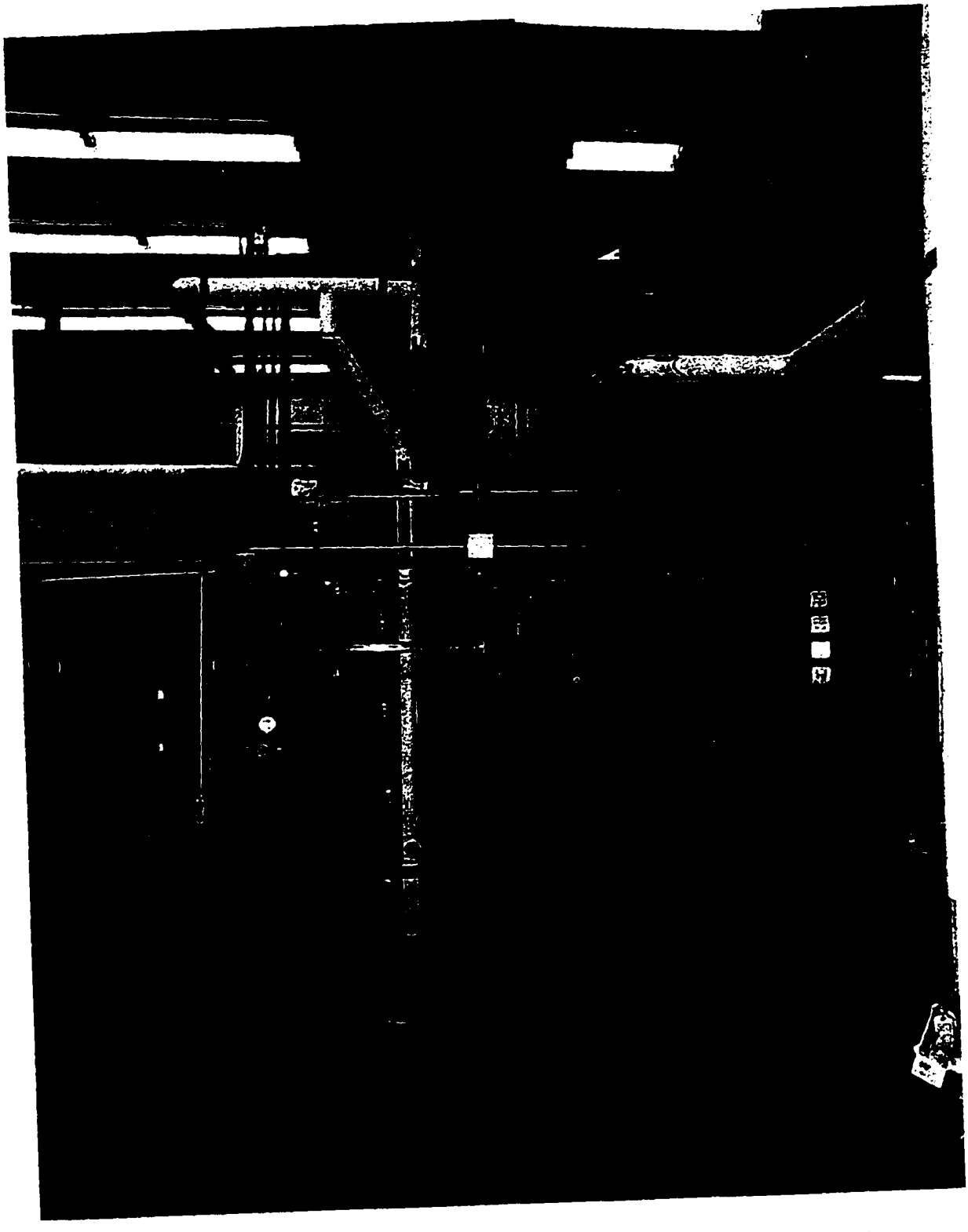

Figure 4. Down-flow reactor with biomass hopper, steam drain, and water jacket.

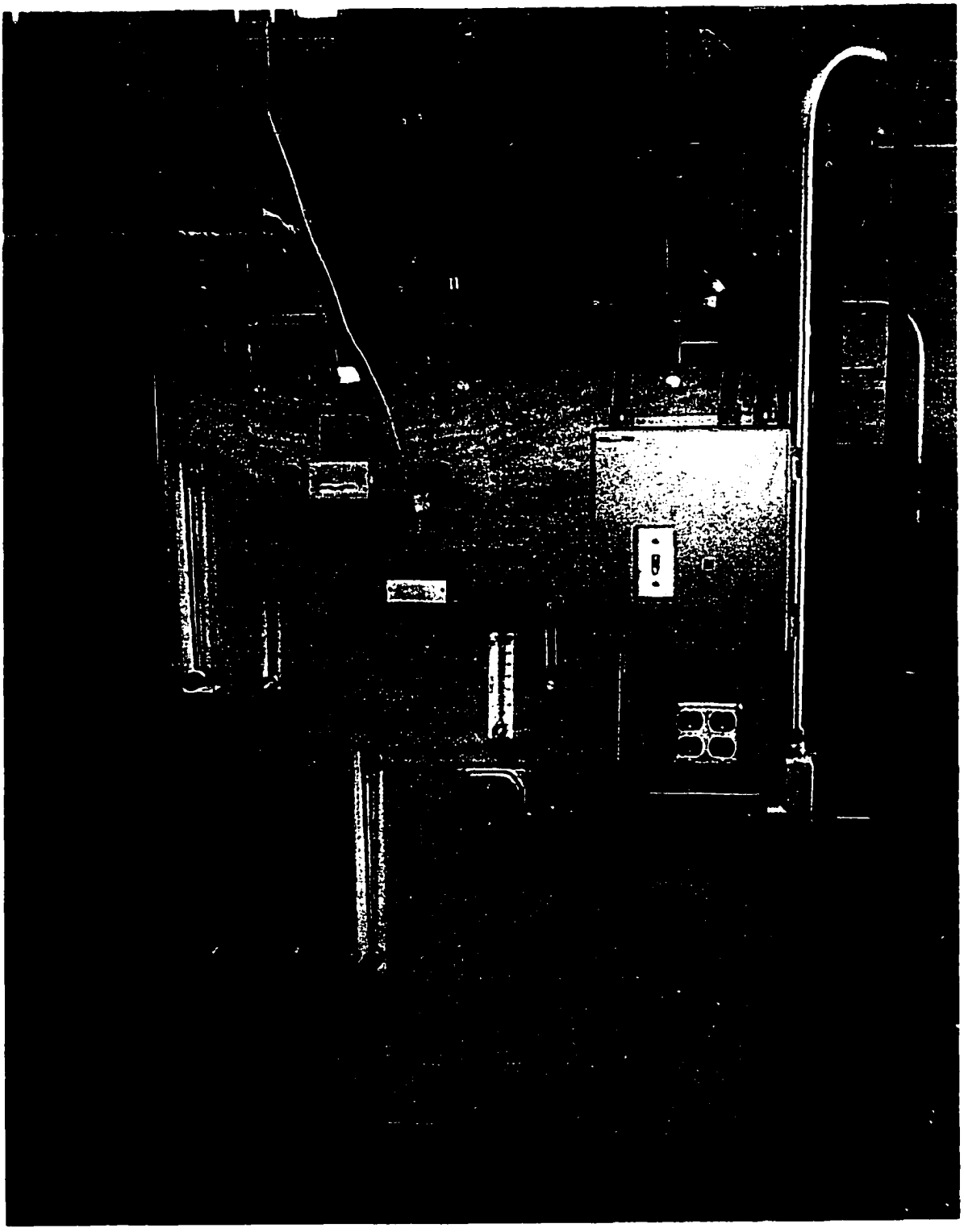

Figure 5. Main control panel.

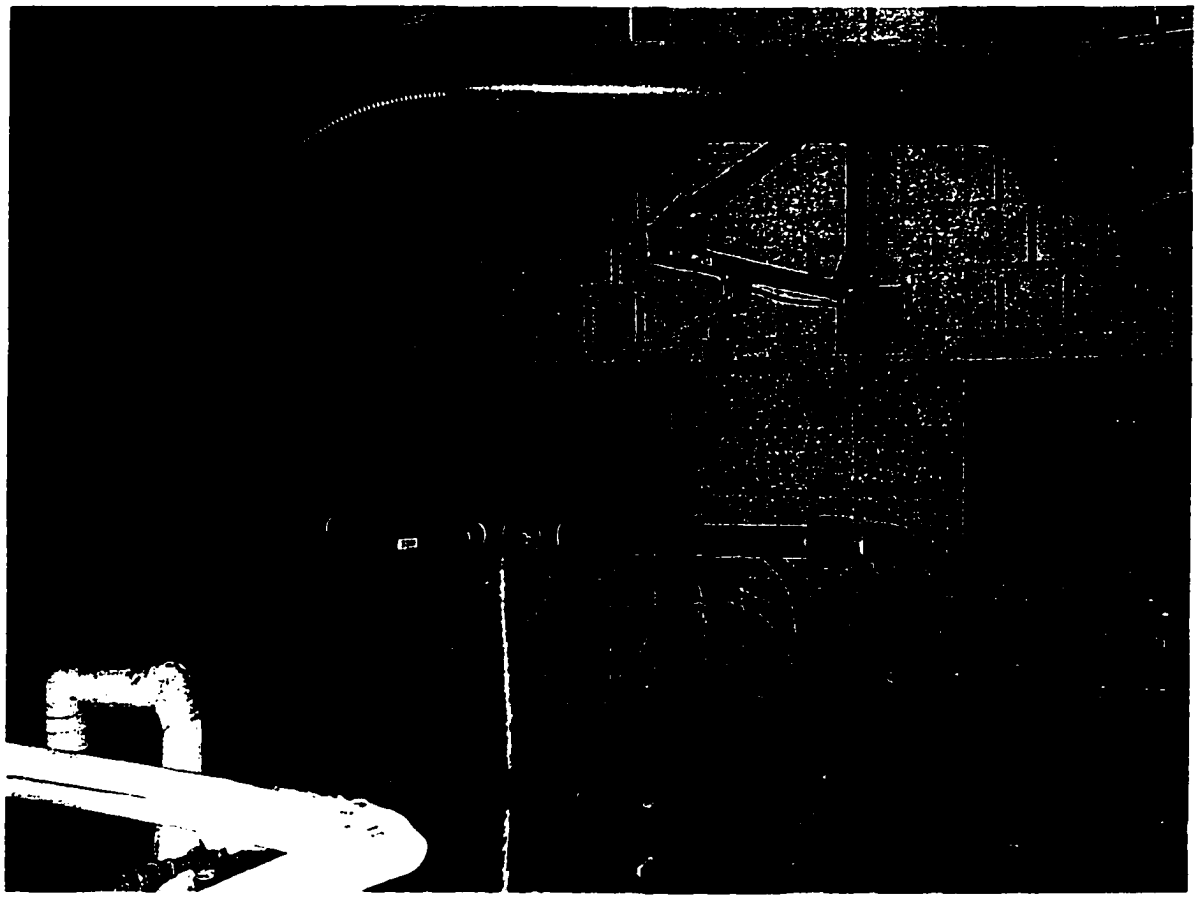

Figure 6. Cyclone, fifth sampling port, and exhaust.

Figure 6 shows how the exhaust from the down-flow reactor is vented from the laboratory. After the process stream leaves the water jacket, it enters a cyclone, pictured on the right of Figure 6, then by the fifth sampling, shown in the middle of Figure 6, and finally is vented to an ceiling fan that exhausts the process stream from the laboratory.

The biomass injection port underwent several modifications. Figure 7 shows the final arrangement. The two most challenging issues were to prevent flue gas in the reactor from entering the biomass hopper and to prevent steam and biomass from forming wet clumps of biomass, which clogged the injection lines. Originally, steam was to be the only carrier gas for the biomass, but it was determined that too much steam was flowing into the biomass

hopper, even when the hopper was sealed. (A perfect seal was never obtained.) Also, the steam was not superheated sufficiently after being throttled through a needle valve to prevent condensation in the horizontal plumbing. Finally, the quantity of steam required to physically transport the biomass from the hopper into the reactor resulted in a significant temperature decrease within the reaction chamber. Mixtures of nitrogen and steam were attempted as transporting gases, but with limited success. The arrangement shown in Figure 7 relies solely on nitrogen as the carrier gas; steam was introduced separately.

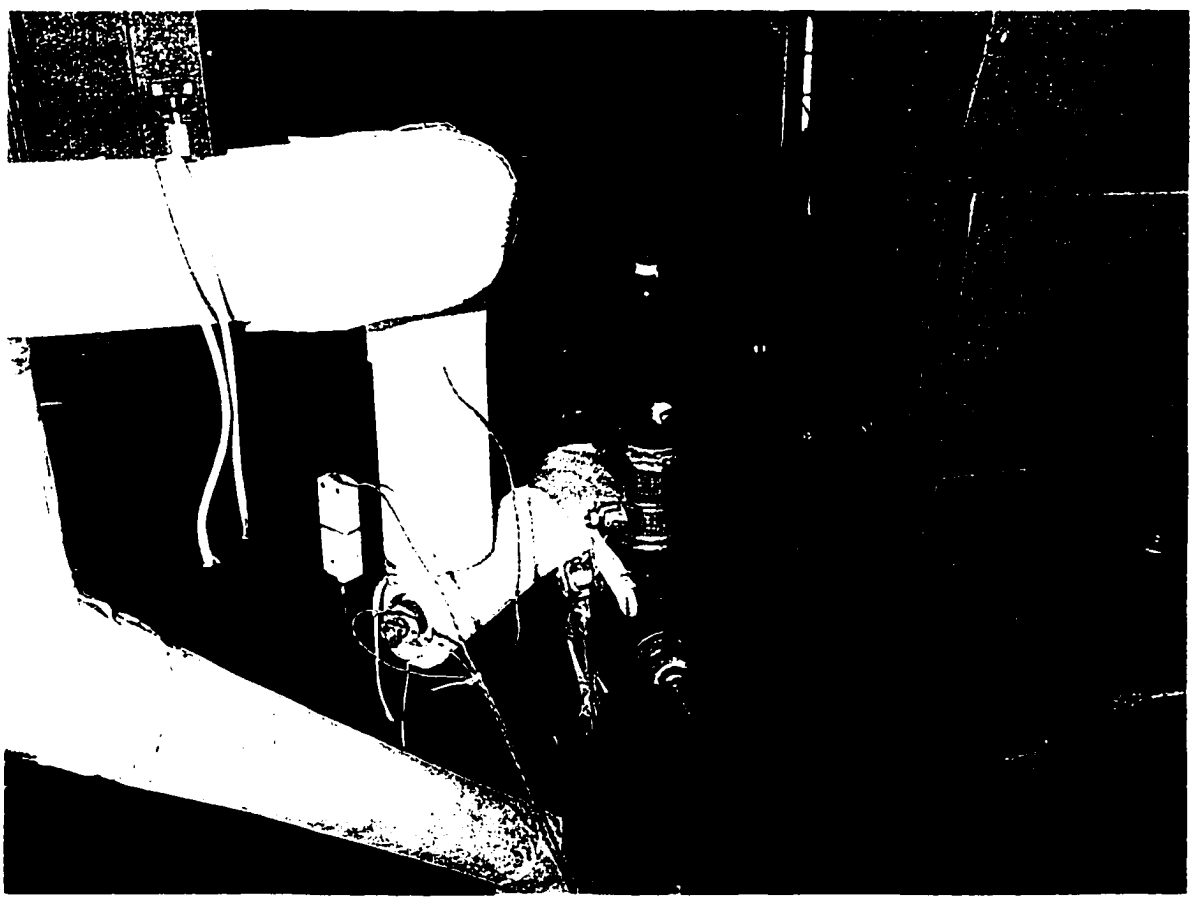

Figure 7. Biomass injection port with steam addition. Nitrogen is injected through the small, brass barbed nipple shown in bottom-center in the figure.

Figure 8 shows the four main sampling ports of the main reaction chamber. The first sampling port is located 1.71 m (67.5 in) from the top of the reactor, or 1.08 m (42.5 in) from the biomass injection port. The residence time from the biomass injection port to this sampling port is estimated to be 0.36 seconds, assuming no biomass or carrier gas is being used. The following three sample ports are each located 0.38 m (15 in) apart. The estimated residence time at the fourth sampling port is 0.81 seconds. The sample line is made of stainless steel tubing and is electrically heated to prevent condensation.

Figure 9 shows the continuous emission gas analyzers, contained in what is referred to as the gas cart. In addition to four separate analyzers, there is a particulate filter, an acid-mist filter, and a PermaPure membrane dryer to condition the gas samples for the analyzers. Oxygen is measured with a California Analytical, Inc., Model 100F electrochemical fuel cell analyzer. Carbon monoxide and carbon dioxide are measured with a California Analytical, Inc., ZRH-2 non-dispersed infrared analyzer. Nitric oxide and nitrogen dioxide are measured in a Thermo Environmental Model 42C-HL chemilumenescient analyzer that is capable of measuring oxides of nitrogen as NO, NO_2, and NO_x. Also in this gas cart is a sulfur dioxide analyzer, although it was not used in this research. All data from the analyzers, as well as from all thermocouples and the digital flow meters, are recorded using National Instruments data acquisition equipment and Labview software. All gas species are reported on a dry basis, unless otherwise noted. CO, CO_2, and NO_x concentrations are corrected to 3% O_2. For example, to correct the CO concentration to 3% O_2, the following equation is used:

$$[CO]_{corrected} = \frac{0.179 \times [CO]_{measured}}{0.209 - [O_2]_{measured}} \qquad (12)$$

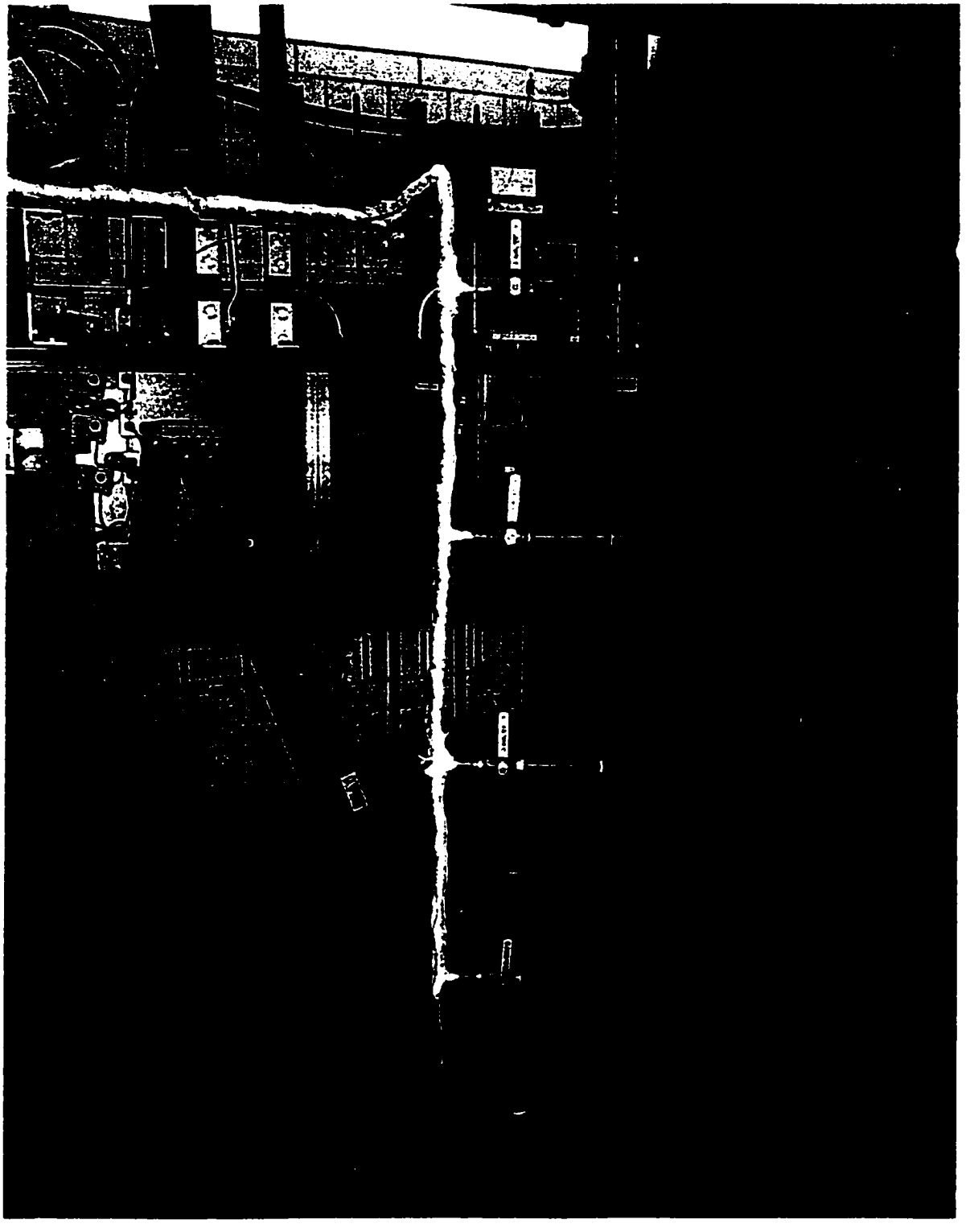

Figure 8. Main sampling ports.

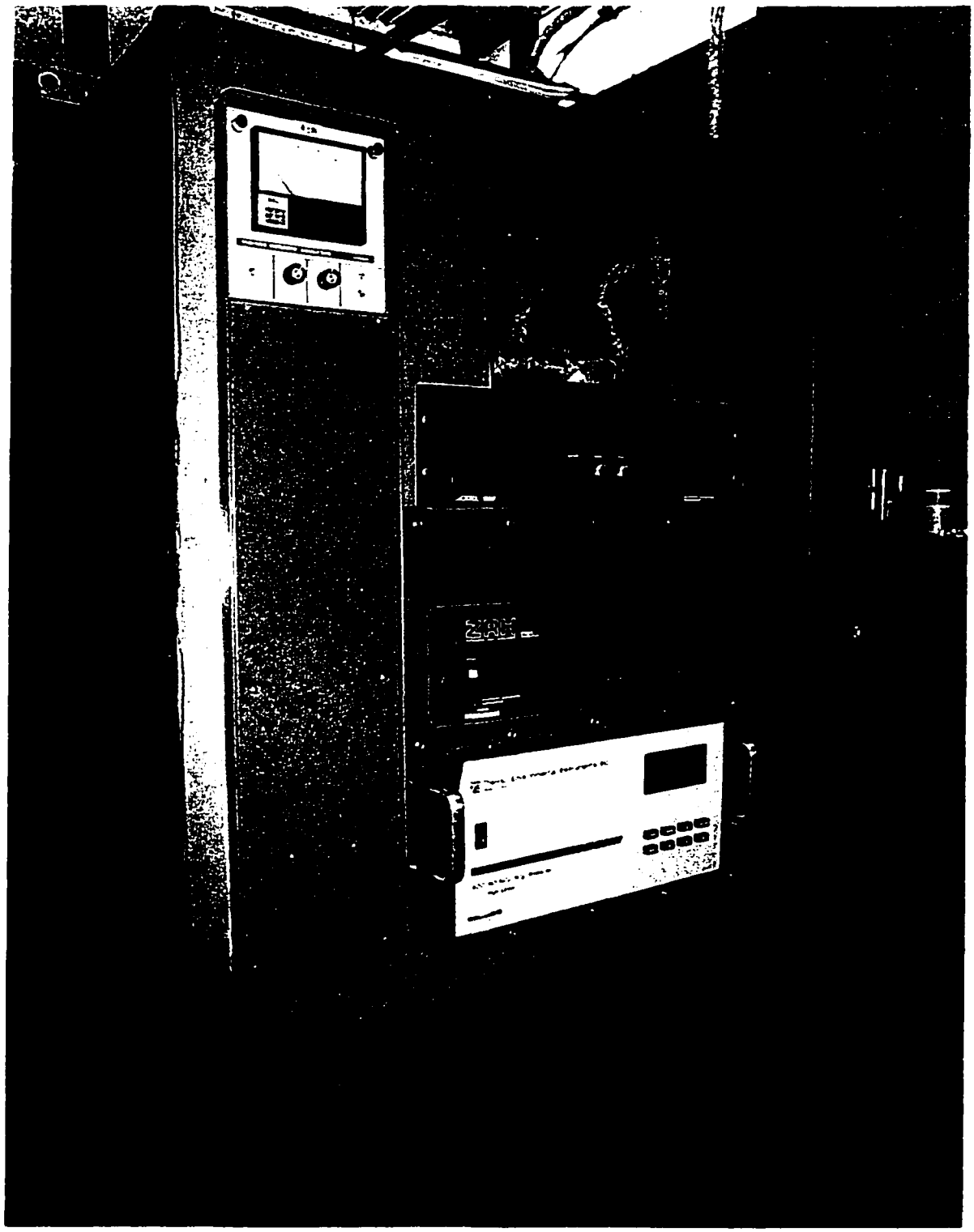

Figure 9. Gas cart that houses all gas analyzers and gas sample conditioning apparatus.

3.2. Summary of Experiments

Four parameters were investigated for this research: 1) the type of carrier gas used, either steam or nitrogen; 2) the amount of biomass used, based on heating value of the biomass; 3) the type of biomass used, either low-nitrogen containing switchgrass or high-nitrogen containing alfalfa; and 4) the initial concentration of oxygen in the flue gas.

A preliminary set of experiments were developed to determine if there would be sufficient mixing of the flue gas with the biomass in the down-flow reactor. Supplementary calculations determined that the Reynolds number within the reactor varied from approximately 2900, near the top of the reactor, to 4300, near the bottom of the reactor. These values indicate only slightly turbulent flow, so there was concern that there may be insufficient mixing between the volatiles coming from the biomass particles and the flue gas. Tracer experiments with carbon dioxide were performed to determine if there were any axial concentration gradients. Radial concentration gradients were not explicitly investigated. Experiments were performed under both hot and cold (room temperature) conditions. At room temperature conditions, lower flow rates of air were required to achieve Reynolds numbers that were comparable to values achieved in the combustor when it was operated hot.

To determine the effect of different carrier gases on the reburning process, a series of experiments were conducted by injecting nitrogen or steam into the reactor without biomass. These tests were important to make sure that subsequent reburning tests with biomass were substantially due to the biomass and not the carrier gas. The combustor was allowed to thermally stabilize during five days of operation. Cylinders of nitrogen were connected to the auxiliary carrier gas rotameter, described previously with Figure 5. Different flow rates of nitrogen were injected into the down-flow reactor through the biomass injection port, and

the axial temperature was measured. To determine the effect of steam addition, a method of injecting a known flow rate of steam was required. Steam available in the laboratory is saturated at 630 kPa (91 psi). To control the flow rate of steam, a precision metering needle valve was installed in the steam line upstream of the biomass injection port. Just upstream of this valve was a branch in the line that allowed the steam to bleed off into a container. This limited the amount of condensation that may collect in the steam line upstream of the needle valve. As the steam exits the needle valve, it is throttled, resulting in superheated, but cooler, steam. A condensing heat exchanger was connected to the steam line to calibrate the steam flow rate, basing the flow rate on the number of complete revolutions of the precision metering needle valve. Zero, two, three, four and five complete turns of the metering valve were tested.

The parameters explored in the reburning experiments included % energy input from biomass, the initial oxygen concentration in the flue gas, and the type of biomass used. The % energy input varied from 4.2% to 23.0%. The initial oxygen concentration in the flue gas varied from 1.05% to 6.35%. Two types of biomass were used, switchgrass and alfalfa. Switchgrass represents a low nitrogen-containing biomass reburn fuel, while alfalfa represents a high nitrogen-containing biomass reburn fuel. The chemical compositions and thermal analyses of switchgrass and alfalfa are presented in Table 1. The average particle size of the groun switchgrass was 0.95 mm, and the particles exhibited a bi-modal size distribution, as shown in Figure 10. The average particle size of the ground alfalfa was 0.77 mm, and the particles exhibited a normal size distribution, as shown in Figure 11.

Table 1. Chemical and thermal analysis of switchgrass and alfalfa.

	Switchgrass		Alfalfa	
	Dry	As Received	Dry	As Received
Proximate				
% ash	3.80%	3.60%	8.45%	7.72%
% moisture		4.10%		8.62%
% volatile matter	82.60%	79.20%	77.80%	71.09%
% fixed carbon	13.60%	13.10%	13.76%	12.57%
Ultimate				
% ash	3.80%	3.60%	8.45%	7.72%
% carbon	44.23%	42.40%	45.95%	41.98%
% hydrogen	5.07%	5.32%	6.01%	6.45%
% nitrogen	0.64%	0.61%	2.92%	2.67%
% sulfur	0.09%	0.09%	0.16%	0.15%
% oxygen	46.17%	47.98%	35.52%	41.03%
MJ / kg (BTU / lb)	18.13 (7793)	17.38 (7470)	18.72 (8050)	17.11 (7356)

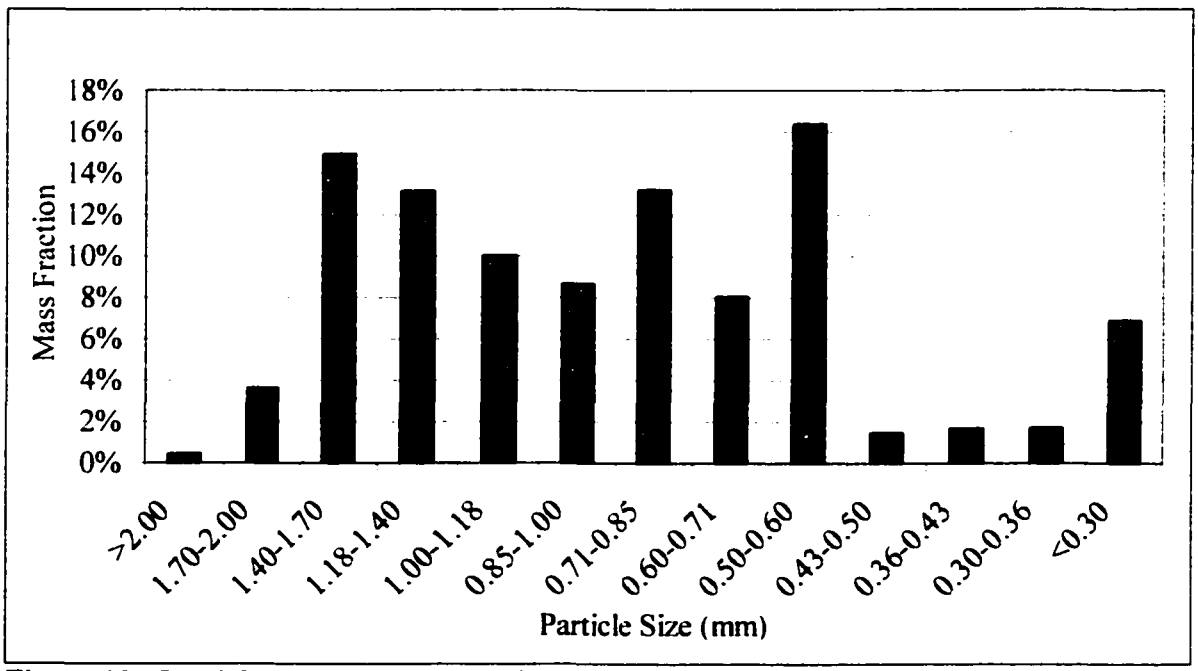

Figure 10. Particle size distribution of ground switchgrass.

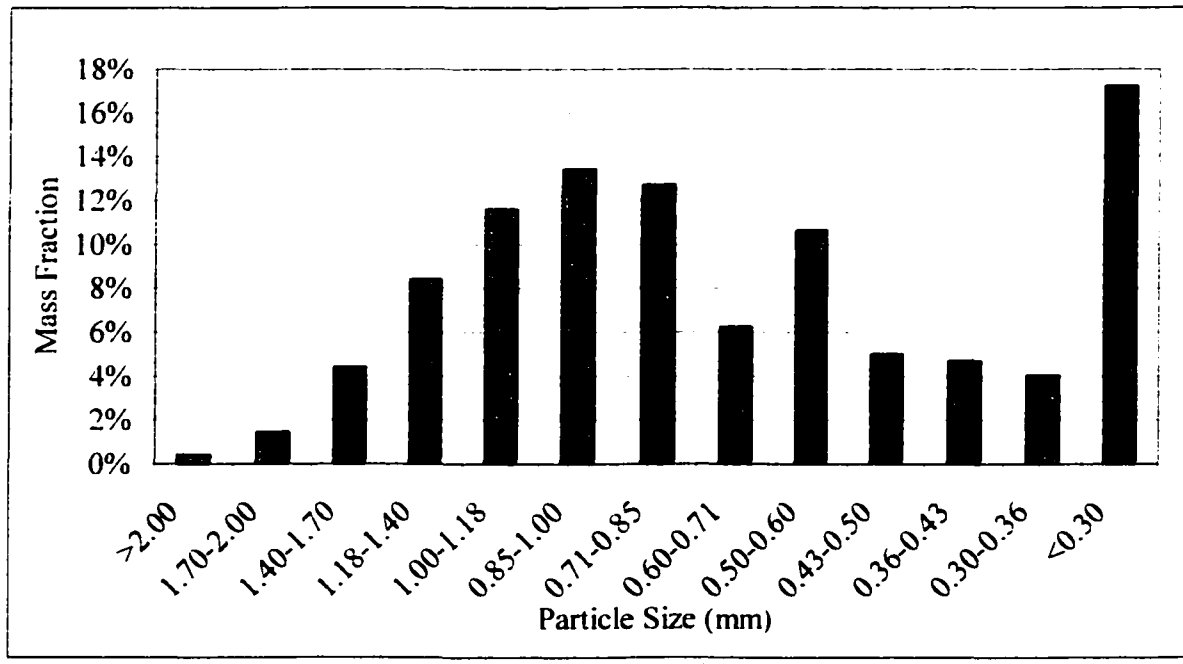

Figure 11. Particle size distribution of ground alfalfa.

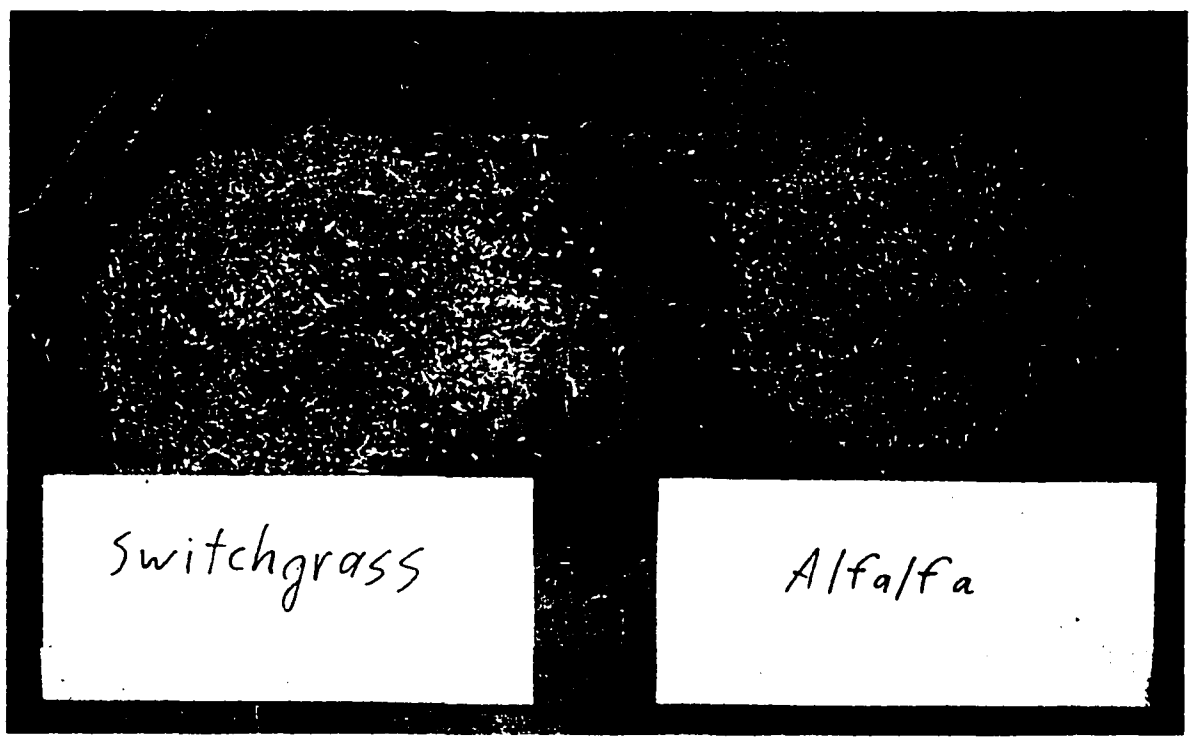

Figure 12. Ground switchgrass and alfalfa.

CHAPTER 4. EXPERIMENTAL RESULTS AND DISCUSSION

4.1. Preliminary Carrier Gas Experiments

To determine the effect of different carrier gases on the reburning process, a series of experiments were conducted by injecting nitrogen or steam into the reactor without biomass. Table 2 summarizes the parameters investigated in the first set of experiments performed, which were designed to determine the effect of nitrogen and steam injection on the initial gas species concentrations. Both nitrogen and steam were introduced into the reactor through the biomass injection port.

NO_x, CO_2, and O_2 concentrations were measured at the exhaust. Figures 13 – 15 show the exhaust concentrations of NO_x, CO_2, and O_2, respectively. For NO_x and CO_2, the only effect of nitrogen injection is dilution. The concentration of O_2, however, remained constant, and no dilution was apparent, which is contrary to what would be expected. The only possible explanation would be that there was a leak in the sample line, drawing air from the surroundings, which could still result in an apparent dilution of other gas species other than oxygen. Figure 16 is the axial temperature profile, measured at locations downstream relative to the biomass injection port, for different flow rates of nitrogen. There was a slight decrease in temperature with increasing amounts of nitrogen, and the profiles become less steep with greater amounts of injected nitrogen. It should be noted that 37.8 L/min of nitrogen injected into the reactor is equivalent to 5.5% of the total mass flow rate in the reactor. For Experiments 13 – 85, however, 47.2 L/min of nitrogen were required to successfully inject biomass into the reactor, but it is thought that additional nitrogen will only

dilute the process stream further without changing the chemistry within the reactor. Error bars in all figures represent the 95% confidence interval.

Figures 17 – 19 show the exhaust concentrations of NO_x, CO_2, and O_2, respectively. In all cases, there was no effect of steam addition, nor any dilution of the analyzed gas stream. This is because the gas conditioning PermaPure membrane dryer removed moisture from the gas sample before it was analyzed. Figure 20 is the axial temperature profile, measured at locations downstream relative to the biomass injection port, for different flow rates of steam. At first steam injection appears have a much greater effect on the axial temperature profile that the nitrogen, but it should be noted that 0.11 kg/min of steam is equivalent to 12.6% of the total mass flow rate within the reactor, which is considerably higher than the 5.5% of the total mass flow rate described earlier for the nitrogen injection experiments.

Table 2. Preliminary carrier gas experiments test matrix. Reactor was operated at 35 kW, with no biomass injection. 0.9% of the total fuel input was anhydrous ammonia.

Experiment	Nitrogen Flow Rate liter / min (SCFH)	Steam Flow Rate g / min
1	0	0
2	18.9 (40)	0
3	28.3 (60)	0
4	37.8 (80)	0
5	0	45
6	0	68
7	0	93
8	0	107

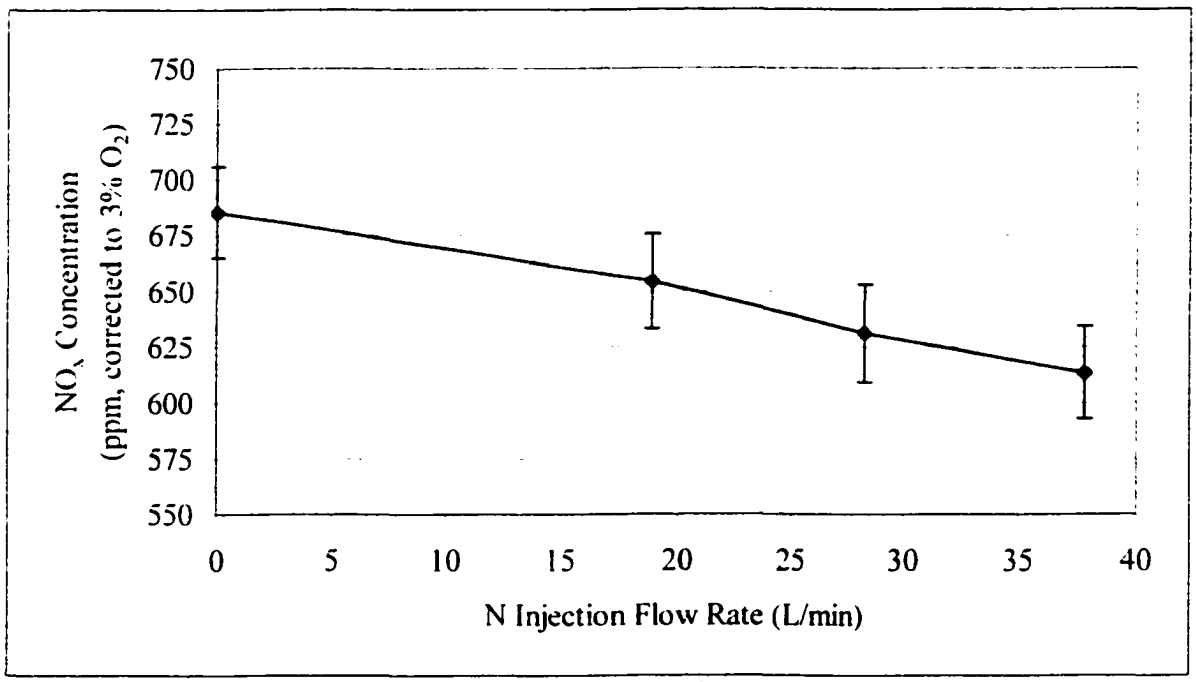

Figure 13. Effect of N_2 injection on NO_x concentration measured at the exhaust. Reactor operated at 35 kW at 3% O_2 with 0.9% of the fuel as ammonia. No steam or biomass was injected.

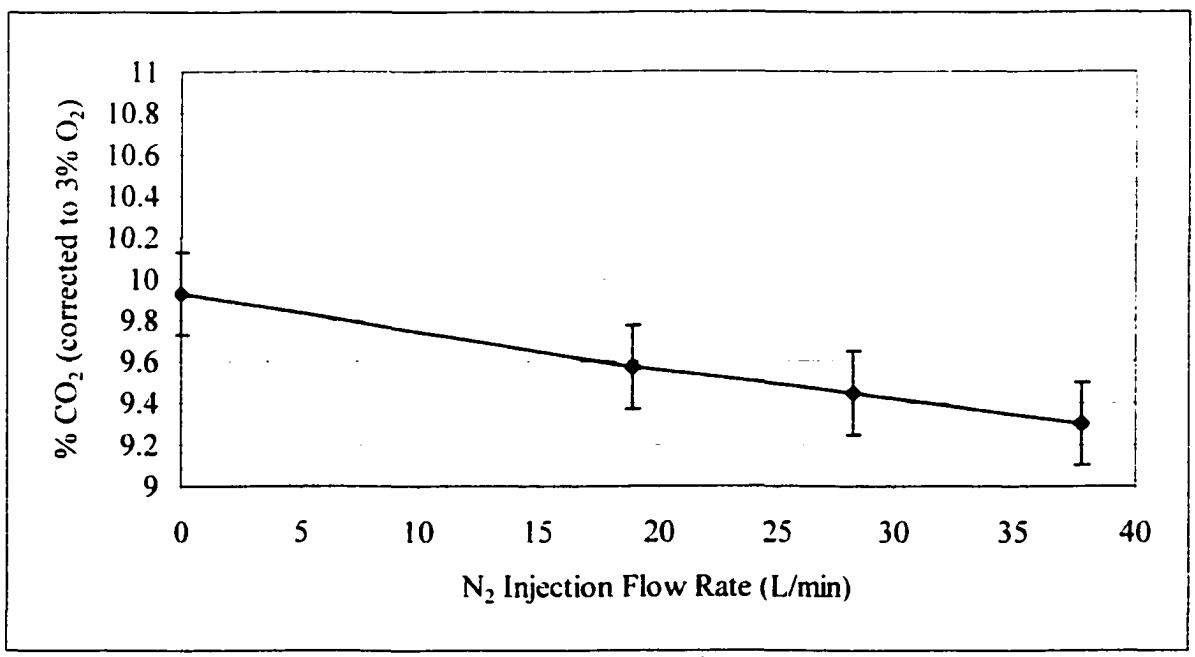

Figure 14. Effect of N_2 injection on CO_2 concentration measured at the exhaust. Reactor operated at 35 kW at 3% O_2 with 0.9% of the fuel as ammonia. No steam or biomass was injected.

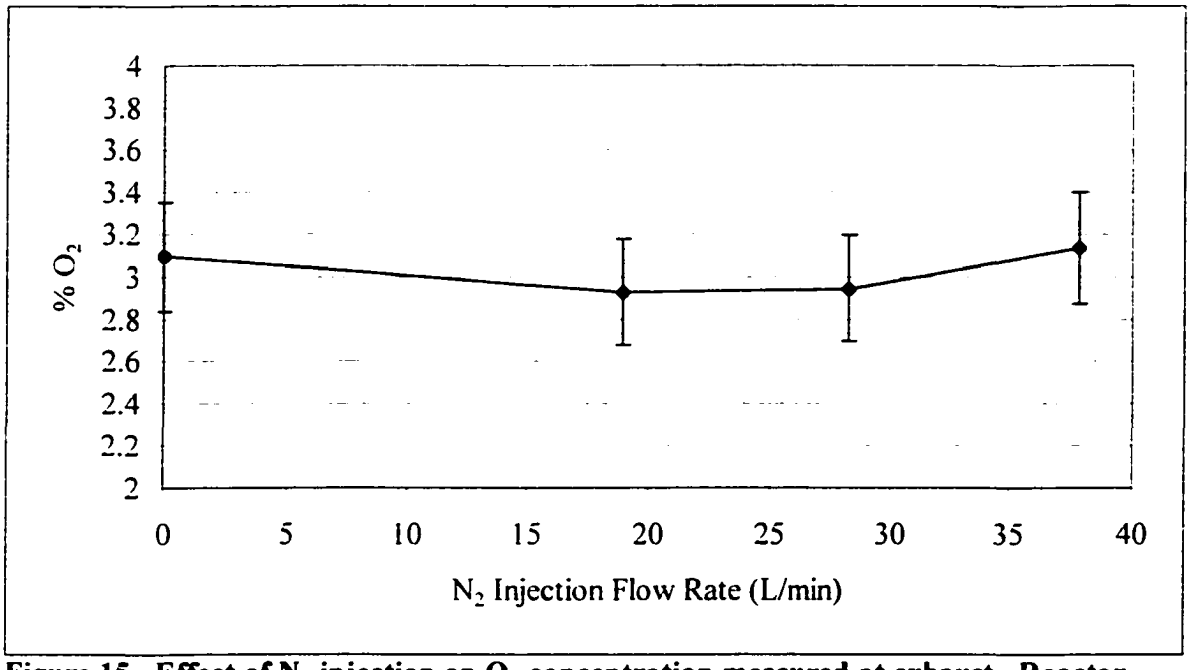

Figure 15. Effect of N_2 injection on O_2 concentration measured at exhaust. Reactor operated at 35 kW with 0.9% of the fuel as ammonia. No steam or biomass was injected.

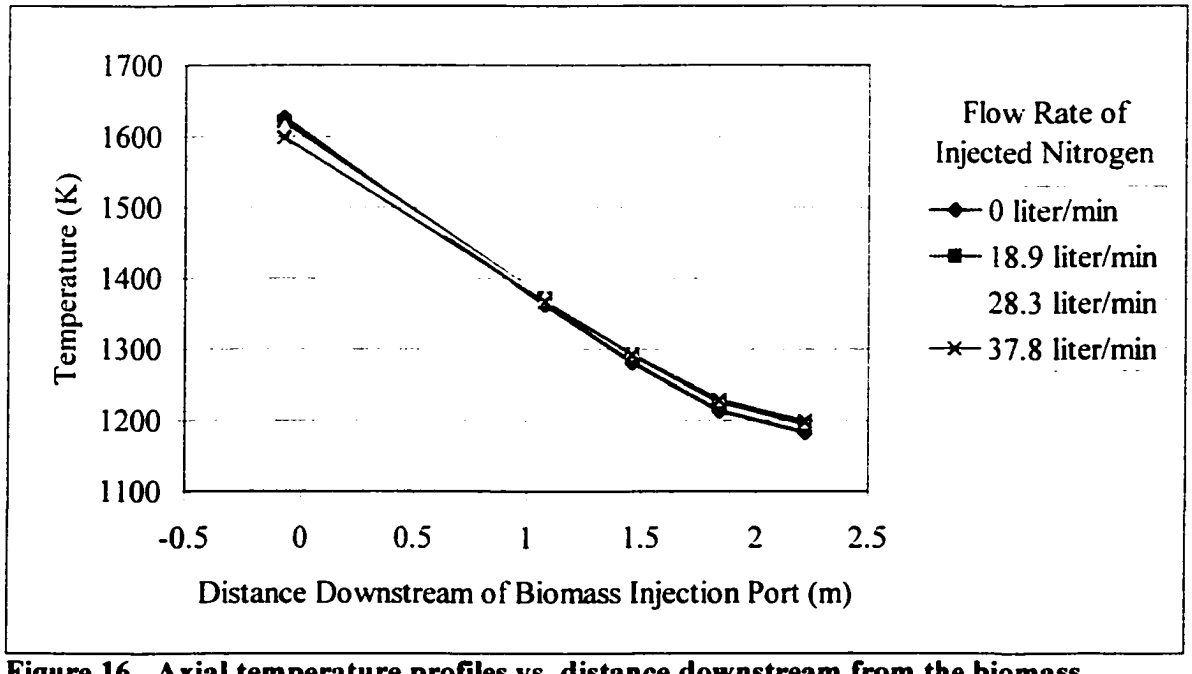

Figure 16. Axial temperature profiles vs. distance downstream from the biomass injection port. Reactor operated at 35 kW at 3% O_2 with 0.9% of the fuel as ammonia. No steam or biomass was injected.

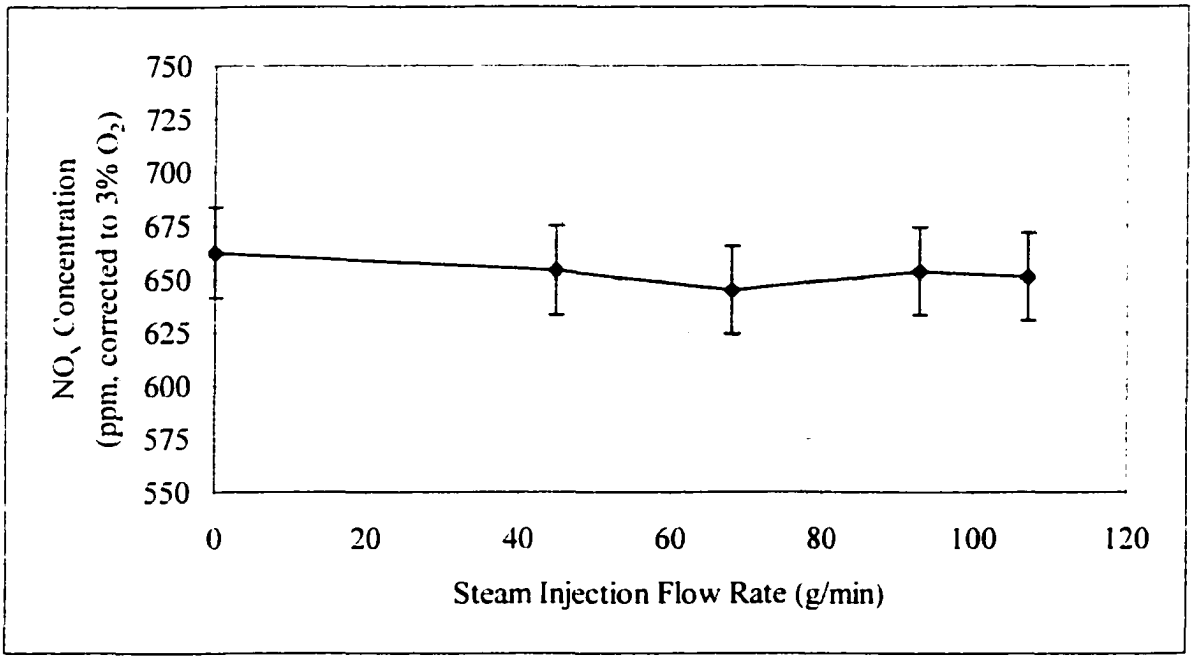

Figure 17. Effect of steam injection on the NO_x concentration measured at the exhaust. Reactor operated at 35 kW at 3% O_2 with 0.9% of the fuel as ammonia. No nitrogen or biomass was injected.

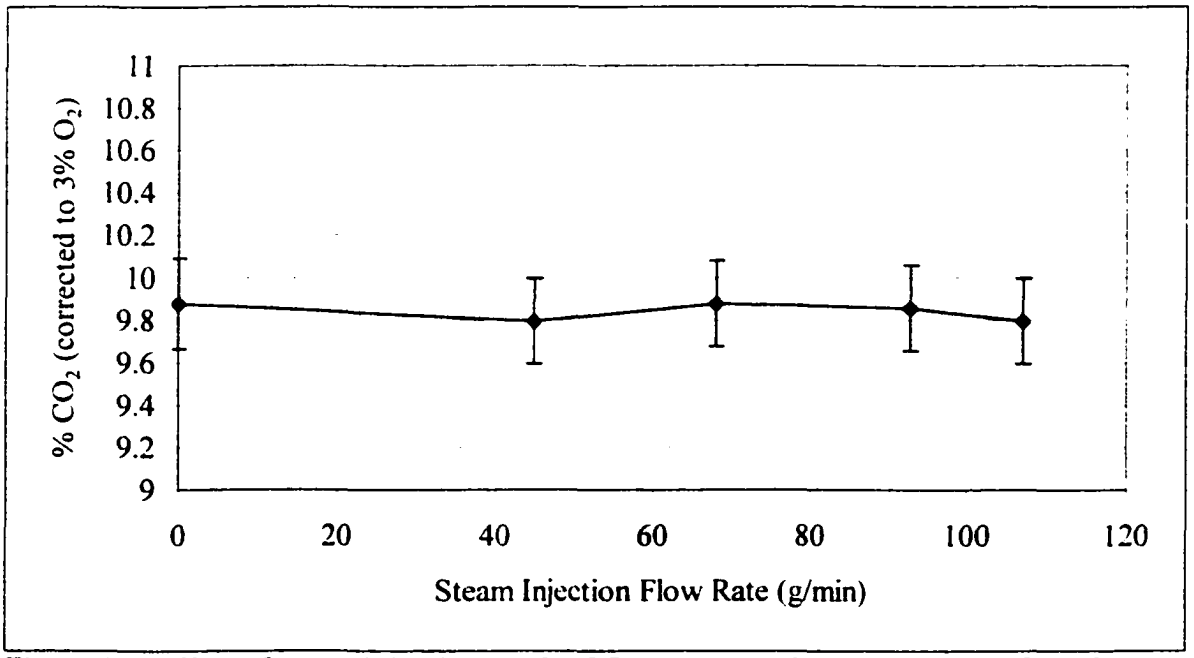

Figure 18. Effect of steam injection on the CO_2 concentration measured at the exhaust. Reactor operated at 35 kW at 3% O_2 with 0.9% of the fuel as ammonia. No nitrogen or biomass was injected.

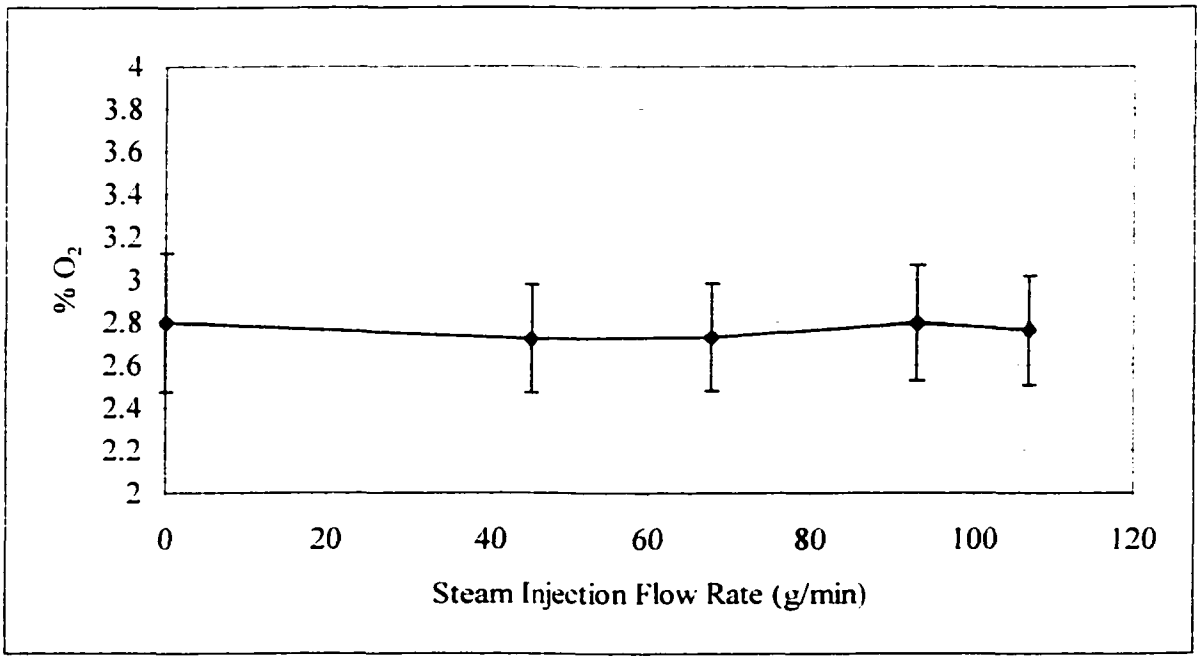

Figure 19. Effect of steam injection on the O_2 concentration measured at the exhaust. Reactor operated at 35 kW with 0.9% of the fuel as ammonia. No nitrogen or biomass was injected.

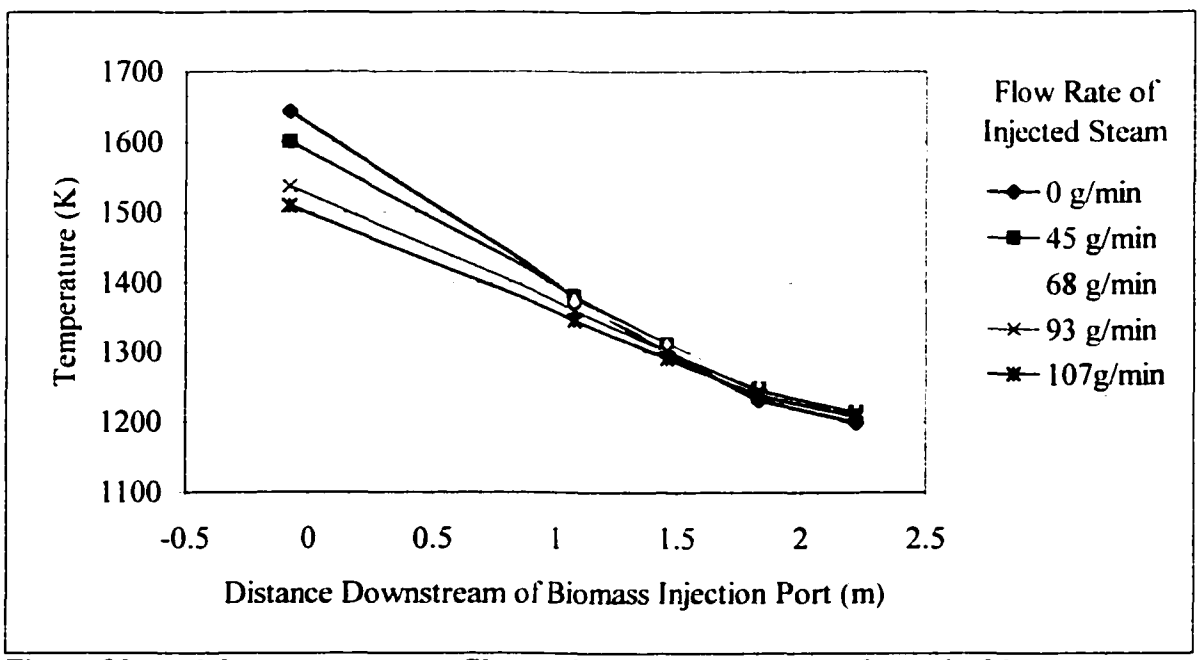

Figure 20. Axial temperature profiles vs. distance downstream from the biomass injection port. No biomass was injected. Reactor operated at 35 kW at 3% O_2 with 0.9% of the fuel as ammonia. No nitrogen or biomass was injected.

Additional experiments with steam demonstrated that the steam flow rate was either unstable or inappropriate for the reburning experiments performed in the laboratory. If a low flow rate of steam was employed, the steam would often cool sufficiently and condense in the plumbing, even though it had been superheated by the throttling process. To prevent condensation, the plumbing would have to be heated or a higher flow rate of steam would be required to keep the plumbing hot. Figure 20 indicates that the higher flow rates of steam significantly impact the axial temperature profile. Attempts to keep the steam super-heated by electrically heating the plumbing downstream of the metering valve where the steam had been throttled were unsuccessful. When steam was used as the only biomass carrier gas, the biomass would clog in a matter of minutes because when the steam came in contact with the room-temperature dry biomass, the steam condensed and was absorbed by the biomass like a sponge. Combinations of steam and nitrogen were tried, but with similar results. Another issue was that the amount of steam required to physically transport the biomass in this particular laboratory environment required a much higher mass flow rate than would be consumed if the biomass were gasified in situ and allowed to react to form hydrogen by the water-gas shift mechanism, as in the following equation:

$$CO + H_2O \leftrightarrow H_2 + CO_2 \qquad (13)$$

CO would come from the gasification of the biomass, and the H_2O would come from the steam, and the H_2 would take part in the reburning process [28]. A 50:50 mixture by mass of steam and biomass would be sufficient to generate hydrogen, but such a mixture was deemed impractical in this small-scale laboratory setting. A larger-scale installation would fare better because the steam could possibly be superheated more effectively, or the plumbing would be larger relative to the biomass particles, or a different injection system could be employed.

Steam was also tried as an additive, with a different plumbing configuration, as shown in Figure 7. With this plumbing configuration, nitrogen was the primary carrier gas, and steam was added to the nitrogen/biomass stream as it entered the reactor. After fifteen minutes of operation, barely enough time to achieve steady-state and not enough time to collect any meaningful data, the biomass would clog inside the flange shown in Figure 7.

4.2. Carbon Dioxide Tracer Experiments

Tracer experiments with carbon dioxide were performed to determine if there were any axial concentration gradients. Radial concentration gradients were not explicitly investigated. These experiments were performed because supplementary calculations determined that the Reynolds number within the reactor varied from approximately 2900, near the top of the reactor, to 4300, near the bottom of the reactor. These values indicate only slightly turbulent flow, so there was concern that there may be insufficient mixing between the volatiles coming from the biomass particles and the flue gas. Table 3 lists the four carbon dioxide tracer experiments that were performed to determine if there was an axial concentration gradient. Both hot and ambient temperature tests were performed. For the ambient temperature tests, the Reynolds number could be controlled because the temperature inside the reactor was constant, resulting in a constant kinematic viscosity and volumetric flow rate throughout the reactor. Two different flow rates of air were used to give two different Reynolds numbers. These Reynolds numbers represent the estimated upper and lower values of the flue gas when the reactor was operating at full power. When the reactor was running under full power, the Reynolds number varied within the reactor because the volumetric flow rate and kinematic viscosity are temperature dependent. Also, unlike the

ambient temperature experiments, there was carbon dioxide in the flue gas prior to carbon dioxide injection, so a baseline had to be established for the hot experiment.

Figures 21 and 22 show the results of the CO_2 tracer experiments, performed to determine if there was sufficient mixing of the injected biomass and the flue gas inside the down-flow reactor. Figure 21 are the results for the room temperature condition, and Figure 22 are the results for when the reactor was at full power. The calculated CO_2 concentrations were determined by performing a mass balance using a set flow rate of CO_2. Instantaneous radial mixing is assumed for these calculations, and any variations of the calculated concentrations are due to fluctuations of the primary air flow rate. The same flow rate of CO_2 was used for both Reynolds numbers. From Figure 21, it can be stated that, within the statistical precision of the experiment, the measured concentration of CO_2 was the same as the calculated concentration, indicating fast radial dispersion of the CO_2 in the air stream. There was no change in concentration axially, which could indicate that the mixing was completed upstream of the first sampling port, or that there might be axial dispersion. Although the absence of axial variations in concentration could be ascribed to rapid axial dispersion, as well, this possibility can be dismissed because of the presence of a temperature gradient.

At room temperature conditions, the residence time was greater between the biomass injection port and the sampling ports because of the lower volumetric flow rate, so there would be more time for the CO_2 to mix with the air. The experiment was repeated when the reactor was running at full power, at 4% O_2, and consequently at a shorter residence time. In Figure 22 baseline concentrations were obtained because, unlike in the previous experiment, there was already some CO_2 present due to combustion of natural gas. The calculated values

were made by assuming complete combustion of natural gas, and instantaneous radial dispersion, with any variations of the calculated values being due to fluctuations of the gas and primary air flow rates. Though the calculated values and the measured values do not correspond as closely as in Figure 21, there is no statistically significant difference between them, indicating again that the CO_2 mixed quickly with the flue gas. There is also no apparent axial concentration profile of CO_2. As mentioned above, this could be due to either complete mixing of the flue gas and the CO_2 upstream of the first sampling port, or due to axial dispersion. Axial dispersion in a tubular reactor would represent a continuously well-stirred reactor, but well-stirred reactors do not have temperature gradients, so it was determined that there is no axial dispersion of the CO_2. From these four experiments it was determined that there was sufficient mixing of CO_2 and flue gas, so there would be sufficient mixing of biomass and flue gas as well, even at these relatively low Reynolds numbers.

Table 3. Carbon dioxide tracer experiments test matrix.

Experiment	Environment	Reynolds Number	Primary Air Flow Rate L / min	Carbon Dioxide Flow Rate L / min
9	Ambient temperature	2900 (estimated lower value)	345	16.9
10	Ambient temperature	4300 (estimated upper value)	515	16.9
11	Reactor operating at 35 kW	Varies within reactor 2900 – 4300		0
12	Reactor operating at 35 kW	Varies within reactor 2900 – 4300		21.1

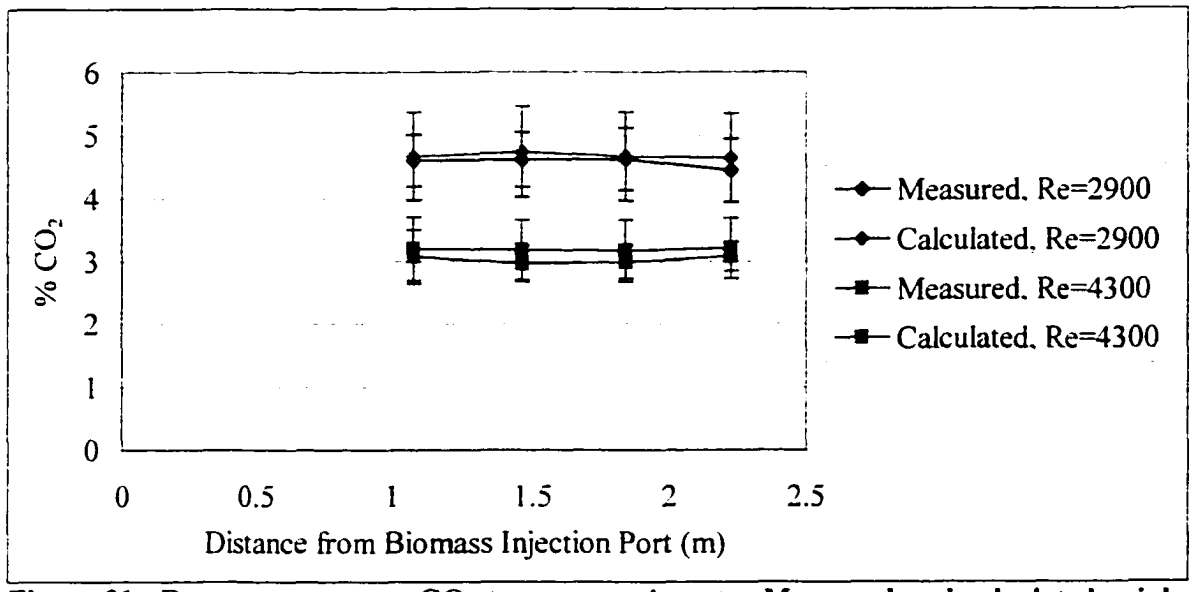

Figure 21. Room temperature CO_2 tracer experiments. Measured and calculated axial CO_2 concentration profiles. 345 L/min of air generated a Reynolds number of 2900, and 515 L/min of air generated a Reynolds number of 4300. 16.9 L/min of CO_2 was injected.

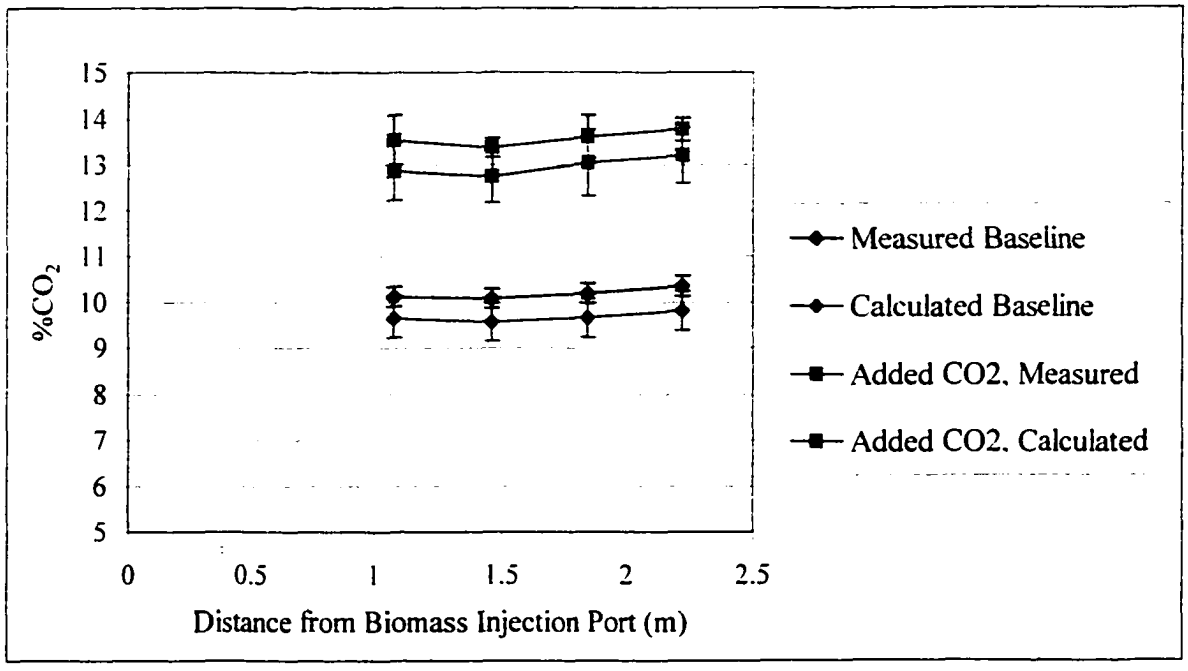

Figure 22. CO_2 tracer experiments when reactor is running at 35 kW at 3% O_2. Measured and calculated axial CO_2 concentration profiles. 21.1 L/min of CO_2 was injected for "Added CO_2" data.

4.3. Computational Fluid Dynamics Modeling

Computational fluid dynamics was used to support the results obtained from the carbon dioxide tracer experiments, and to demonstrate that there is no significant radial concentration gradient within the reactor. A computer model of the reactor geometry was generated with the software package GAMBIT™ [26]. There were three different regions within the geometry of the down-flow reactor that were modeled: 1) the fluid region, 2) the ceramic insulation, and 3) the silicon carbide burner tube. The sampling ports, thermocouple probes, the view port, and the water jacket were not included in the geometry for simplicity. The steel shell of the reactor was also excluded from the geometry because a significant temperature gradient was expected through the 0.23 m (9 in)-thick insulating ceramic. The temperature gradient through the steel shell was assumed to be comparatively small. Figure 23 is the wire-frame representation of the down-flow reactor. The flow enters the reactor through the small vertical chamber at the top (the silicon carbide burner tube) and exits out the bottom and to the right. At the bottom and to the left in the figure is the ash access port. Near the top of the figure is where biomass and nitrogen is injected.

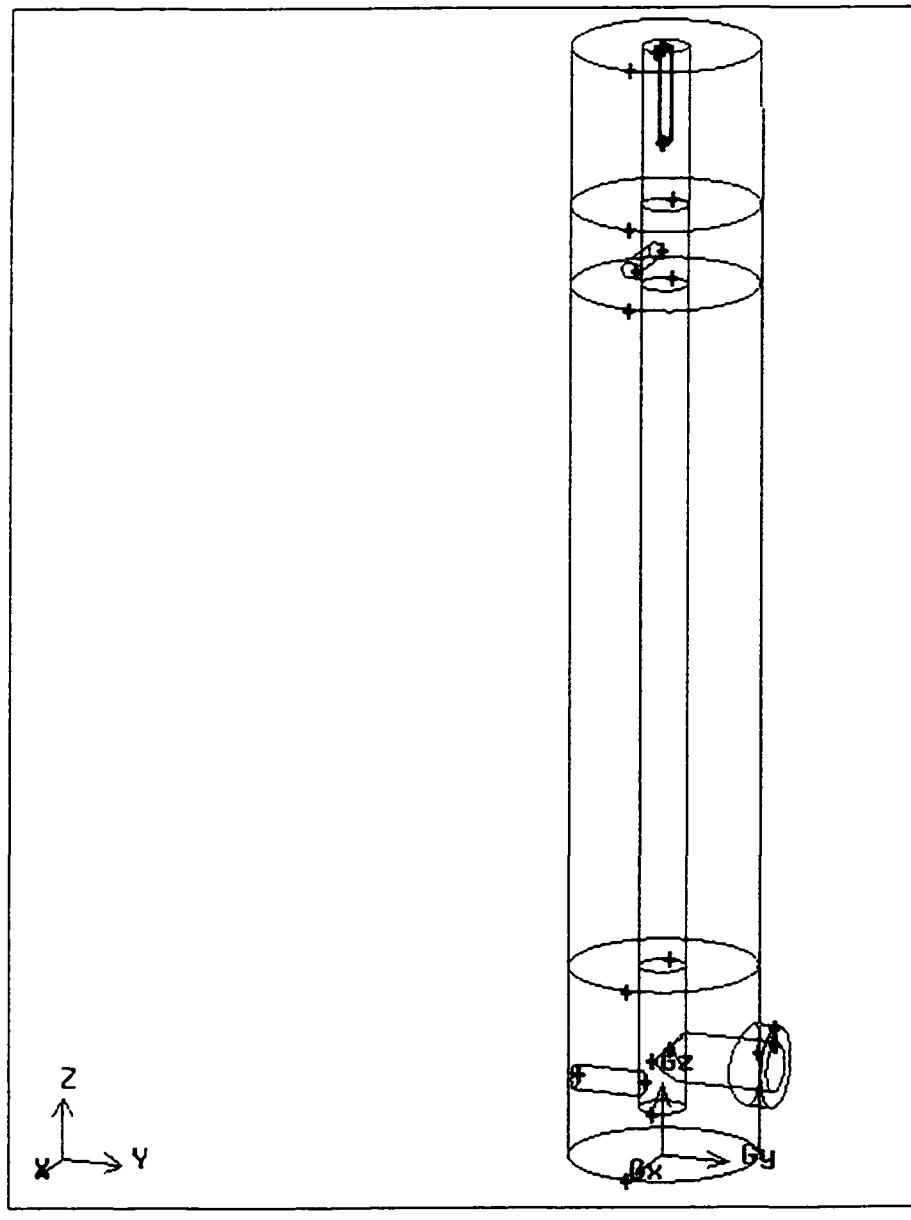

Figure 23. Wire-frame representation of the down-flow combustor.

Hot air enters the model through the small vertical cylinder shown at the top of the figure, and nitrogen and biomass are injected through the horizontal chamber shown near the top of the figure. The small horizontal chamber shown near the bottom-left of the model is where ash would collect, and at the bottom right of the model is where the fluid exits the model. 168,751 nodes were generated for the down-flow reactor, and this geometry and meshing scheme data was imported into FLUENT™ [26], the software package that performs the desired numerical calculations.

Several parameters had to be set before FLUENT™ could solve the continuity, momentum, energy, turbulence, and species equations. The reactor model was simulated in three dimensions under steady-state conditions using the k-ϵ model for turbulence [27]. Default values for relaxation factors, the discretization scheme, and solution limits were used. Details of the types of modeling used and the solver controls are presented in Appendix C.

Constant physical properties were used for the fluids. Silicon carbide and ceramic were not part of the FLUENT™ database of available materials, so their properties had to be incorporated into the database. Heat capacity and thermal conductivity for ceramic, as well as the thermal conductivity of silicon carbide, were provided by their manufacturers with specific values at specific temperatures. From this data for these materials, curve-fitting software was used to generate first-order temperature-dependent polynomials for the ceramic, and the heat capacity of the silicon carbide was approximated as a second-order temperature-dependent polynomial. Details of the material properties can be found in Appendix C.

Air at 1600 K was introduced into the reactor in the amount of 11.7 kg/s (600 liter/min) through the silicon carbide burner tube, while 9×10^{-4} kg/s (100 scfh) of nitrogen at 300 K was introduced into the reactor through the biomass injection port. Experimental work had shown that the surface temperature of the reactor was nearly constant for the entire height of the reactor, so the outer surface temperature of the reactor model was kept constant at 400 K. The reactor was operated under atmospheric pressure in the simulations.

Figures 24 – 27 are images of the oxygen concentrations generated by FLUENT™ at an elevation within the reactor equal to the sampling ports. Nitrogen was injected approximately 1 m upstream of the first sampling port in the negative-x direction (note orientation of x-y-z axes in the corner of each figure). From the figures one can determine that there is some slight variation of the oxygen concentration at each sampling port. At Sampling Port 1, the oxygen concentration ranged from 19.05% to 19.70% while at Sampling Port 4 the oxygen concentration ranged from 19.20% to 19.55%. These variations (± 0.33% for Sampling Port 1, ± 0.18% for Sampling Port 4) can be compared with the experimental error of the carbon dioxide tracer experiments of approximately 0.5% (note the error bars in Figures 21 and 22). Though the computational fluid dynamics modeling predicts a radial concentration gradient within the reactor at the elevations of the sampling ports, the gradient is smaller than what could be detected experimentally, so from an experimental point of view, the flue gas is well mixed within the reactor.

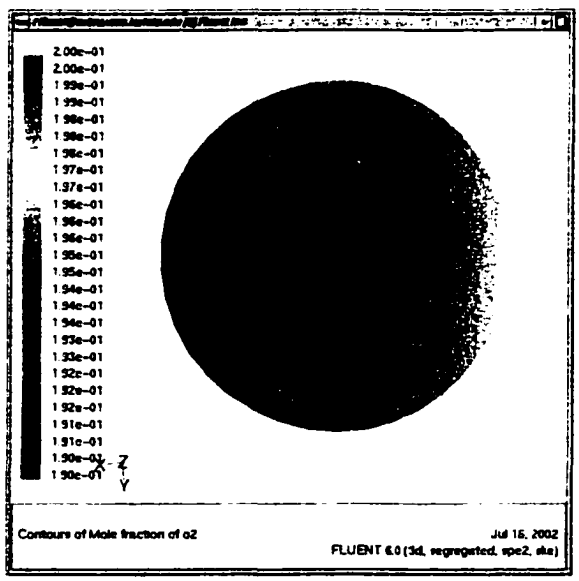

Figure 24. Radial oxygen concentration at Sampling Port 1. Nitrogen was injected upstream of this location from the left.

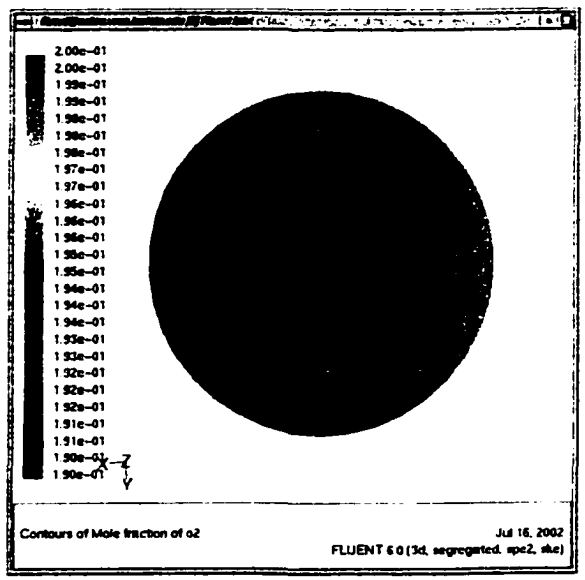

Figure 25. Radial oxygen concentration at Sampling Port 2.

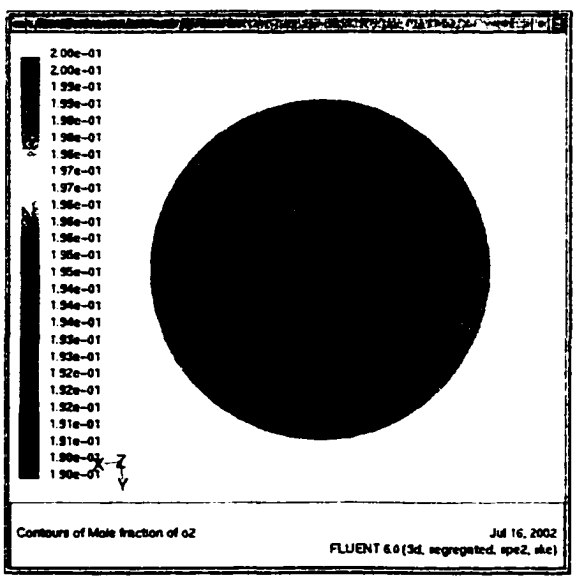

Figure 26. Radial oxygen concentration at Sampling Port 3.

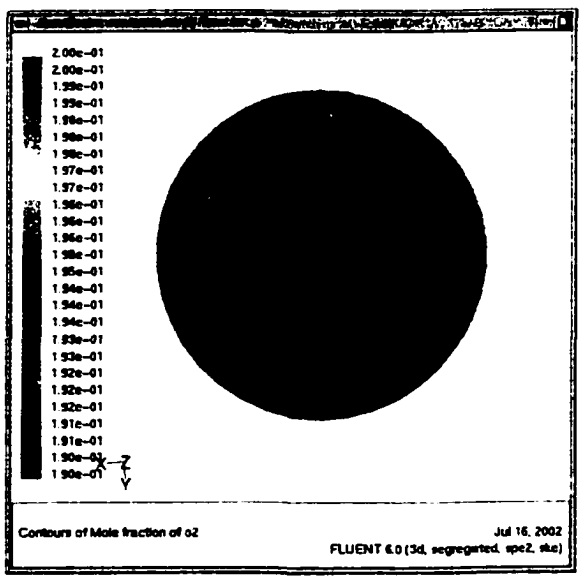

Figure 27. Radial oxygen concentration at Sampling Port 4.

4.4. Fuel-Lean Biomass Reburning Experiments

The following sets of experiments were performed to determine what optimum % energy input from biomass, initial oxygen concentration in the flue gas, and type of biomass would result in the highest percentage of NO_x reduced while maintaining low (>100 ppm) concentrations of CO. Table 4 is the list of reburn experiments that were performed using switchgrass as the reburn fuel. In all experiments, 47.2 L/min (100 scfh) of nitrogen was used as the carrier gas. The O_2 concentration varied from 1.14% to 3.93% for simulated pulverized coal boilers (Experiments 13 – 37) and from 4.91% to 6.35% (Experiments 38 – 51) for simulated stoker boilers. The initial NO_x concentration, was 507 ± 33 ppm. The % energy input from biomass varied from 0.0% – 19.3%. Table 5 is the list of reburn experiments that were performed using alfalfa as the reburn fuel. The initial O_2 concentration varied from 1.05% to 3.96% for simulated pulverized coal boilers (Experiments 52 – 73) and from 4.91% to 6.35% (Experiments 74 – 85) for simulated stoker boilers. The initial NO_x concentration was 502 ± 38 ppm. The % energy input from biomass varied from 0.0% to 23.0%.

Table 4. Switchgrass reburn experiments test matrix.

Experiment	Initial Oxygen Concentration (% vol.)	Switchgrass Flow Rate (g / min)	% Energy Input From Switchgrass
13	1.14	0.0	0.0
14	1.14	5.5	4.2
15	1.14	9.1	6.7
16	1.14	12.6	9.1
17	1.14	16.2	11.3
18	1.73	0.0	0.0
19	1.73	5.5	4.2
20	1.73	9.1	6.7
21	1.73	12.6	9.1
22	2.94	0.0	0.0
23	2.94	5.5	4.2
24	2.94	9.1	6.7
25	2.94	12.6	9.1
26	2.94	16.2	11.3
27	2.94	19.7	13.5
28	2.94	23.3	15.5
29	3.93	0.0	0.0
30	3.93	5.5	4.2
31	3.93	9.1	6.7
32	3.93	12.6	9.1
33	3.93	16.2	11.3
34	3.93	19.7	13.5
35	3.93	23.3	15.5
36	3.93	26.9	17.5
37	3.93	30.4	19.3
38	4.91	0.0	0.0
39	4.91	5.5	4.2
40	4.91	9.1	6.7
41	4.91	12.6	9.1
42	4.91	16.2	11.3
43	4.91	19.7	13.5
44	4.91	23.3	15.5
45	6.35	0.0	0.0
46	6.35	5.5	4.2
47	6.35	9.1	6.7
48	6.35	12.6	9.1
49	6.35	16.2	11.3
50	6.35	19.7	13.5
51	6.35	23.3	15.5

Table 5. Alfalfa reburn experiments test matrix.

Experiment	Initial Oxygen Concentration (% vol.)	Alfalfa Flow Rate (g / min)	% Energy Input From Alfalfa
52	1.05	0.0	0.0
53	1.05	6.6	6.7
54	1.05	14.3	10.5
55	1.05	21.6	14.0
56	2.06	0.0	0.0
57	2.06	6.6	6.7
58	2.06	14.3	10.5
59	2.06	21.6	14.0
60	2.06	27.5	17.2
61	3.07	0.0	0.0
62	3.07	6.6	6.7
63	3.07	14.3	10.5
64	3.07	21.6	14.0
65	3.07	27.5	17.2
66	3.07	31.6	20.2
67	3.96	0.0	0.0
68	3.96	6.6	6.7
69	3.96	14.3	10.5
70	3.96	21.6	14.0
71	3.96	27.5	17.2
72	3.96	31.6	20.2
73	3.96	37.9	23.0
74	4.91	0.0	0.0
75	4.91	6.6	6.7
76	4.91	14.3	10.5
77	4.91	21.6	14.0
78	4.91	27.5	17.2
79	4.91	31.6	20.2
80	6.35	0.0	0.0
81	6.35	6.6	6.7
82	6.35	14.3	10.5
83	6.35	21.6	14.0
84	6.35	27.5	17.2
85	6.35	31.6	20.2

Figures 28 and 29 compare the final NO_x concentrations using switchgrass and alfalfa as reburn fuels. One reason these two biomasses were selected because of their different nitrogen content. Normally, a low-nitrogen containing fuel would be used as the reburn fuel, as is the case of switchgrass. Alfalfa, however, with its much higher nitrogen content, could possibly be a useful reburn fuel as well because the nitrogen in the alfalfa could be released as amino-compounds, which would assist the reburning process [28]. For an initial O_2 concentration of 1%, both biomasses reduced NO_x. However, switchgrass injection reduces NO_x concentrations for 2%, 3%, and 4% O_2, while alfalfa injection generates NO_x until more than 12% of the energy input is from alfalfa for 2% O_2 and more than 17% of the energy input is from alfalfa for 3% O_2. For the stoker boiler simulations when the reactor operated at 5% and 6% O_2, switchgrass injection had no effect on the NO_x concentration, but alfalfa injection increased the NO_x concentration. The desired effect of amine enhancement was not achieved, rather it was determined that the fuel-bound nitrogen in the alfalfa was being oxidized

Figures 30 and 31 compare the % NO_x reduction using switchgrass and alfalfa as reburn fuels, which is simply a reorganization of the data presented in Figures 28 and 29. In this format, one can determine that for an initial O_2 concentration of 1%, NO_x reductions of up to 70% are possible with 12% – 15% of the energy input from the reburn fuel. For higher oxygen concentrations, more switchgrass is required to achieve appreciable NO_x reduction, but $\%NO_x$ reductions are not as high (for initial O_2 concentrations of 5% or greater, no $\%NO_x$ reduction was obtained). When alfalfa is used with higher initial O_2 concentrations, the nitrogen in the alfalfa is oxidized, increasing the NO_x concentration, until a large fraction of the energy input is from the reburn fuel. These differences in $\%NO_x$ reduction between

switchgrass and alfalfa indicate that switchgrass was an effective reburn fuel, while alfalfa generated NO_x.

Figures 32 and 33 compare the final CO concentrations using switchgrass and alfalfa as reburn fuels. Significantly less CO was produced by alfalfa injection than by switchgrass injection. No appreciable quantities of CO were formed under the very fuel lean conditions of 5% and 6% O_2. The large error bars are due to unsteady biomass injection, which is a result of the pulsating nature of the biomass-metering auger. From Figures 30 and 32, one can estimate that the best NO_x reduction while maintaining low CO emissions is 20% – 25% when operating at 11% energy input from switchgrass for 3% O_2 in the flue gas to 16% energy input for 4% O_2 in the flue gas. Alfalfa reduced NO_x emissions only under fuel-rich conditions.

As described previously, in a full-scale boiler there would radial concentration gradients and several turbulent eddies of different NO_x, O_2, and CO concentrations. As these turbulent eddies mix downstream, the CO and O_2 would mix, allowing for additional CO to be further converted to CO_2, but because the temperatures are lower, there would be less chance of the NO_x concentration to increase when nitrogen in one eddy mixes with oxygen from another. Results from this phenomena would be that CO concentration would be lower, on average, than from the experiments performed in this research.

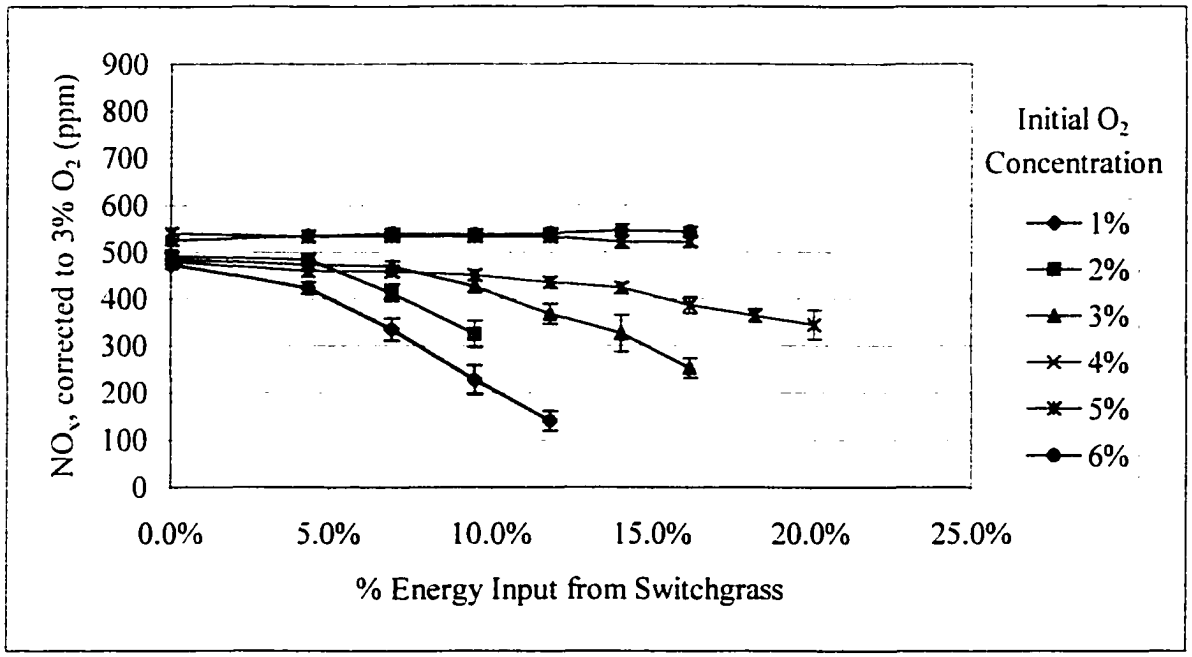

Figure 28. Final NO_x concentrations vs. % energy input from switchgrass.

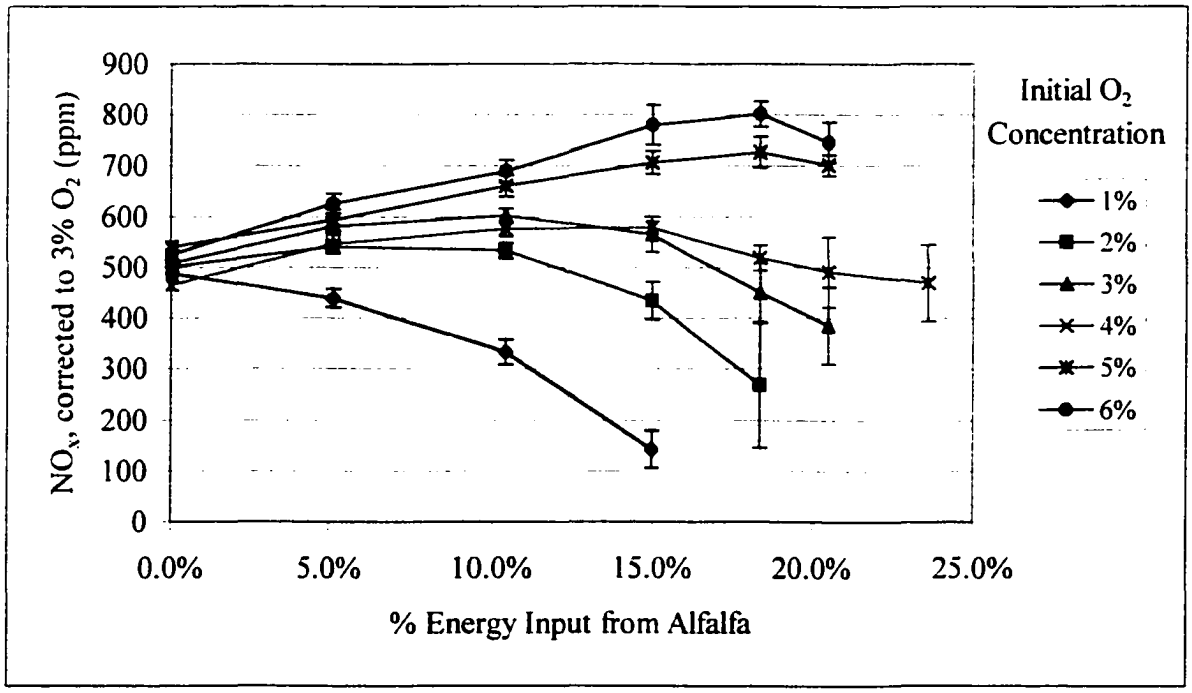

Figure 29. Final NO_x concentrations vs. % energy input from alfalfa.

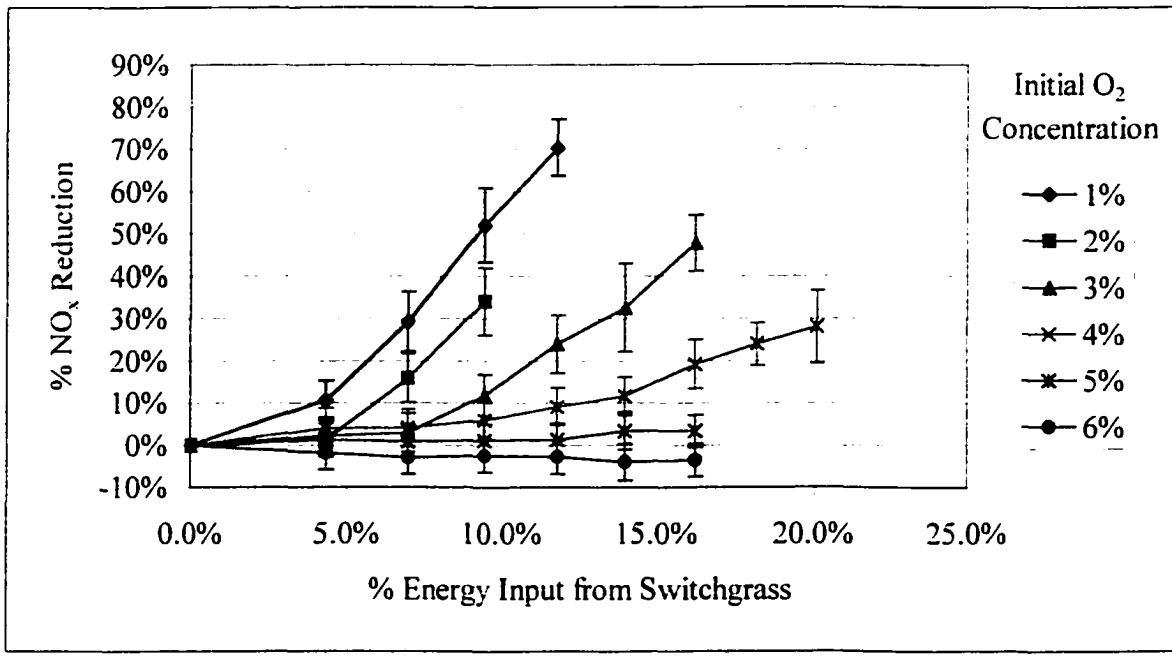

Figure 30. % NO_x reduction vs. % energy input from switchgrass. Negative values indicate NO_x generation.

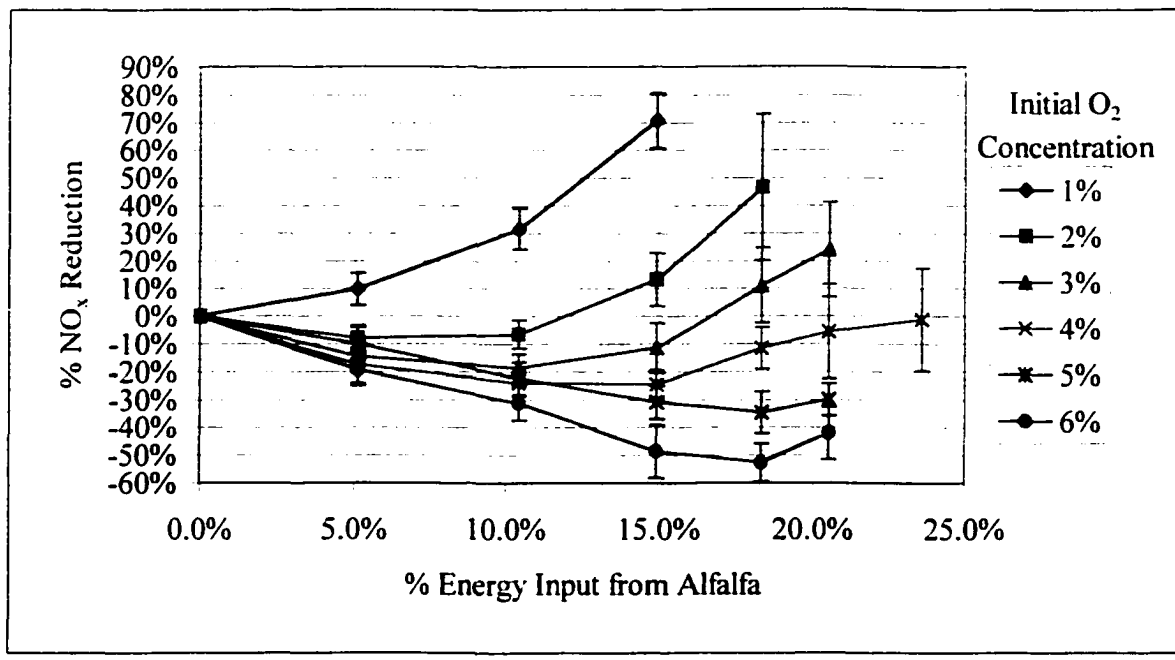

Figure 31. % NO_x reduction vs. % energy input from alfalfa. Negative values indicate NO_x generation.

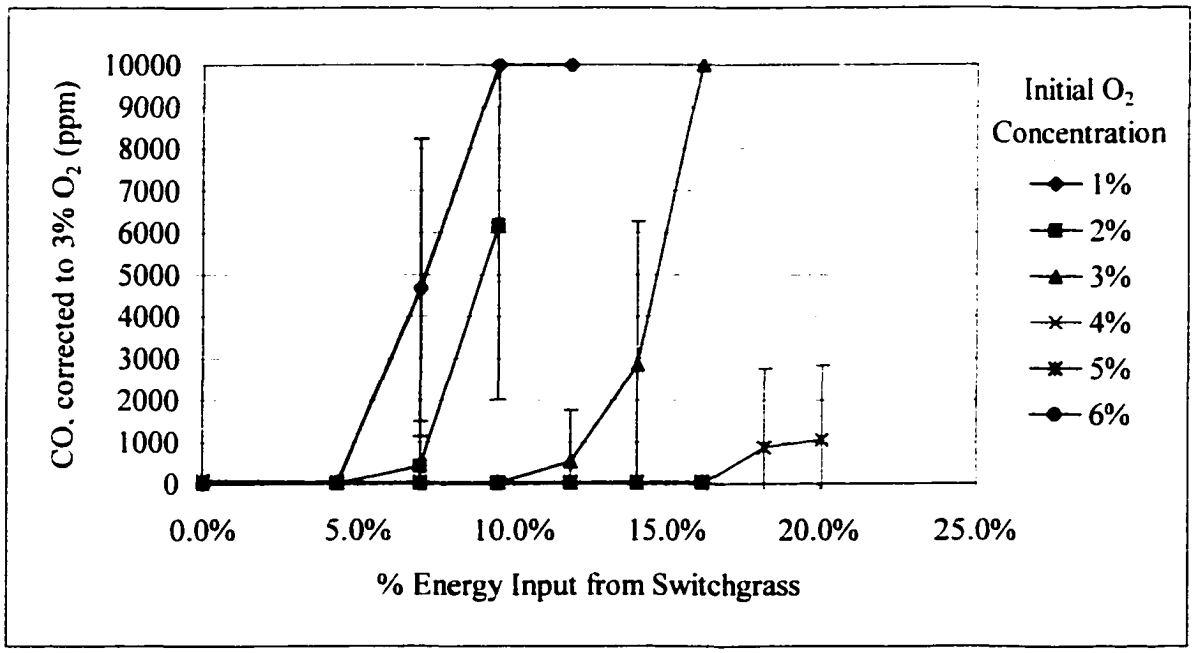

Figure 32. Final CO concentrations vs. % energy input from switchgrass.

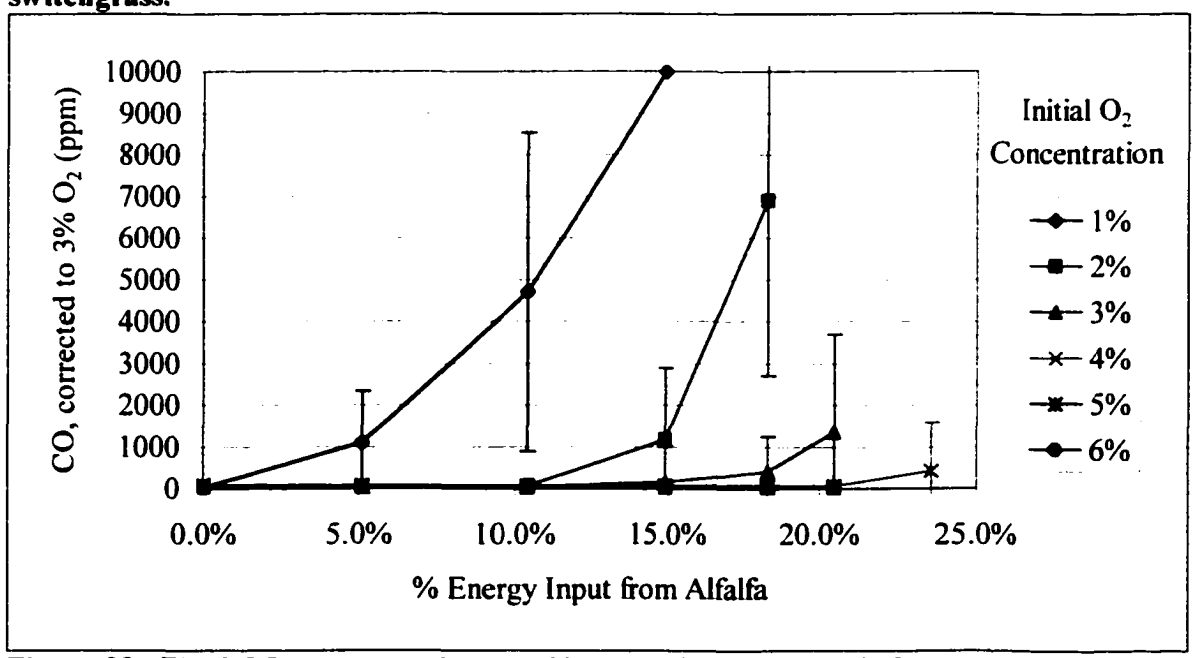

Figure 33. Final CO concentrations vs. % energy input from alfalfa.

Figures 34 – 36 are representative temperature profiles in the down-flow reactor for initial concentrations of 1%, 3%, and 6% O_2 using switchgrass as the reburn fuel. Figure 34 shows the addition of biomass does not significantly increase the temperature at the point of injection, and the temperature downstream increases marginally when operating with an initial O_2 concentration of 1%. The reactor becomes fuel-rich, limiting how much energy can be obtained from the combustion of biomass because the combustion is incomplete.

Figure 35 shows the addition of biomass increases the temperature when operating with an initial O_2 concentration of 3%. More energy is released from the addition of switchgrass because there is sufficient oxygen to react with it. The baseline temperature, 0% energy input from switchgrass, is lower than for the 1% O_2 experiments.

To obtain an initial O_2 concentration of 6%, the mass flow rate of air was 22% higher than the 3% O_2 operating condition while maintaining a constant natural gas flow rate. Comparatively, to obtain an initial O_2 concentration of 3%, the mass flow rate of air was only 11% higher than the 1% O_2 operating condition, with a constant flow rate of natural gas. Figure 36 shows that because of this high flow rate of air for the 6% O_2 operating condition (and a higher flow rate of flue gas), the addition of biomass has less of an effect on temperature profiles. The baseline temperatures are much lower than for the previous two figures, and the temperature profiles are less steep, which indicates that the gas stream is cooling at a slower rate. Temperature profiles for alfalfa were similar.

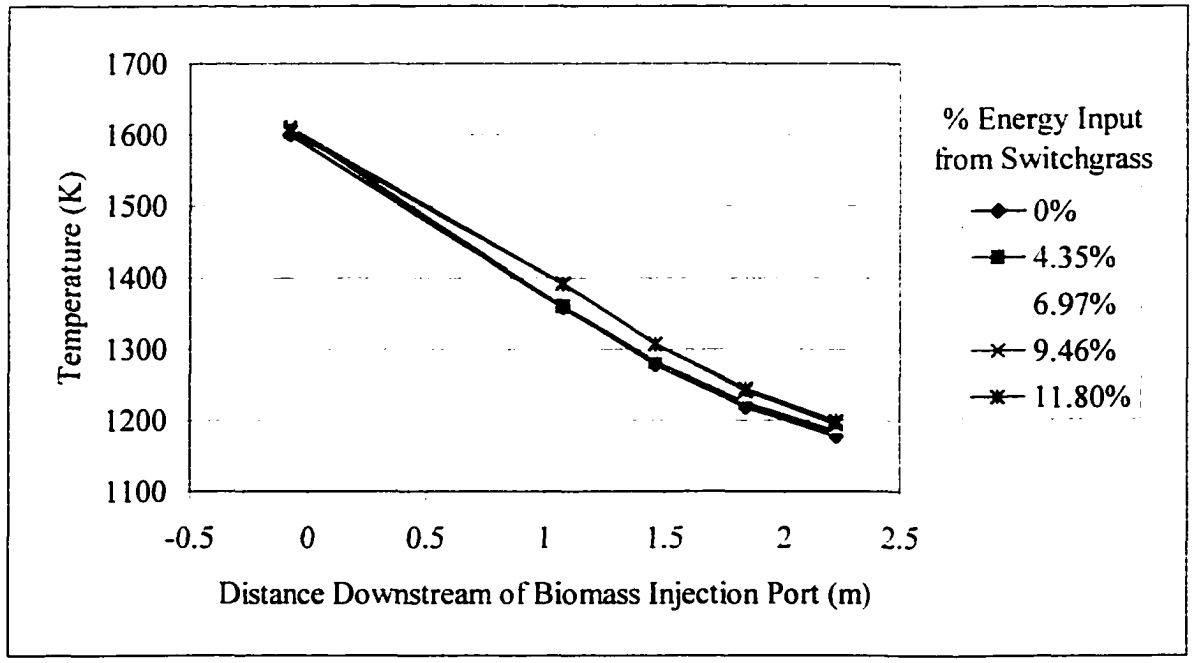

Figure 34. Axial temperature profiles. Distance is downstream from biomass injection port. 1% initial O_2.

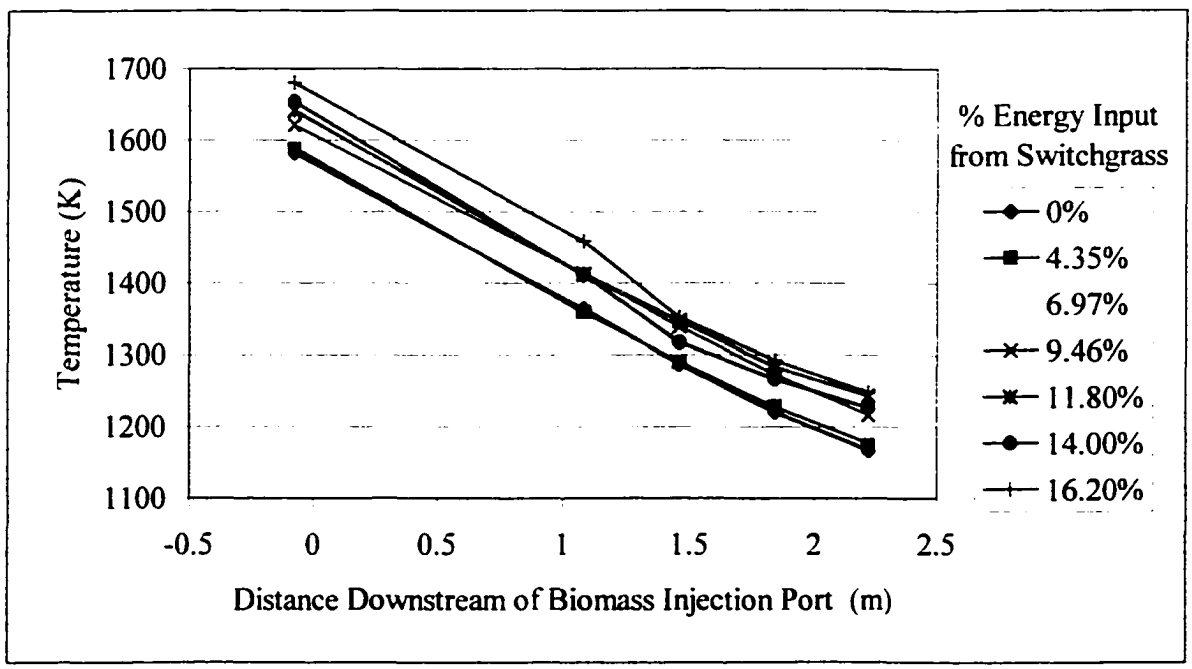

Figure 35. Axial temperature profiles. Distance is downstream from biomass injection port. 3% initial O_2.

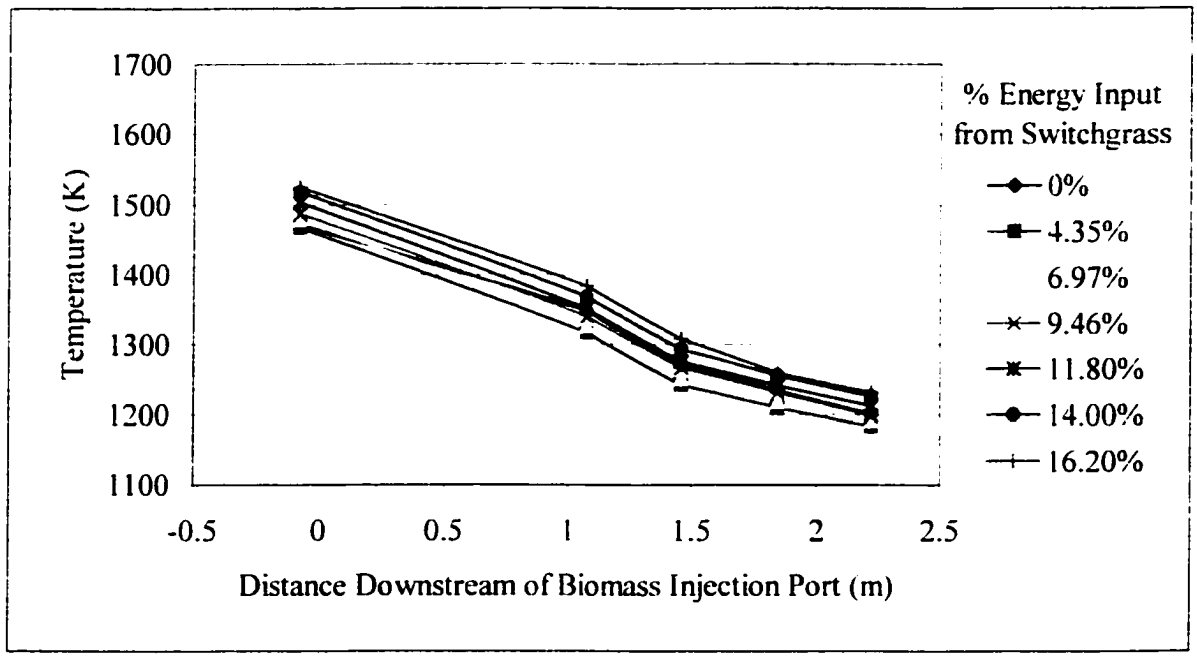

Figure 36. Axial temperature profiles. Distance is downstream from biomass injection port. 6% initial O_2.

CHAPTER 5. CONCLUSIONS

5.1. Experimental conclusions.

Four parameters of Fuel-Lean Biomass Reburning were investigated in this research: the type of carrier gases used to inject the biomass into the down-flow reactor, the initial oxygen concentration, the % energy input from the reburn fuel, and the type of biomass used.

Both nitrogen and steam were tested as the biomass carrier gas, and neither influenced the baseline chemistry inside the down-flow reactor. Additional experiments demonstrated that there was a lack of precise control of the steam flow rate, resulting in either too much steam or not sufficiently hot steam, and in either case the biomass clogged the plumbing. Nitrogen was a much more consistent carrier gas.

Mixing experiments demonstrated that even at the relatively low Reynolds numbers achieved in the laboratory, the injected biomass would mix with the flue gas sufficiently to react with NO_x in the flue gas. Computational fluid dynamic modeling indicated that radially mixing of gas and biomass would be rapid, a result confirmed by mixing experiments.

Switchgrass proved to be better than nitrogen-rich alfalfa as a reburn fuel. There appeared to be no amine enhancement by using alfalfa. At low initial O_2 concentrations, both switchgrass and alfalfa managed to reduce NO_x emissions, but produced high CO emissions. For moderate initial O_2 concentrations, 20% – 25% NO_x reduction was possible for switchgrass while maintaining low CO emissions, but the addition of alfalfa increased the NO_x concentration due to oxidation of the fuel-bound nitrogen present in alfalfa for most initial O_2 concentrations. For high initial O_2 concentrations, which were present in the stoker boiler simulations, there was no appreciable effect on the NO_x concentrations when switchgrass was injected.

5.2. Future work.

There are several additional approaches to modeling Fuel-Lean Biomass Reburn, both experimentally and computationally. Experimentally, different initial NO_x concentrations should be studied, as there may be limitations to how low a typical quantity of NO_x could be reduced; higher initial concentrations of NO_x may be able to be reduced by a larger percentage than what was used in this research. If the reactor was sufficiently large enough, the biomass could be targeted to specific regions within the reactor, creating a more realistic scenario than modeling individual eddies.

APPENDIX A: SCHEMATICS OF ASSEMBLED STEEL SHELL OF THE DOWN-FLOW REACTOR

Assembled Large Spacer

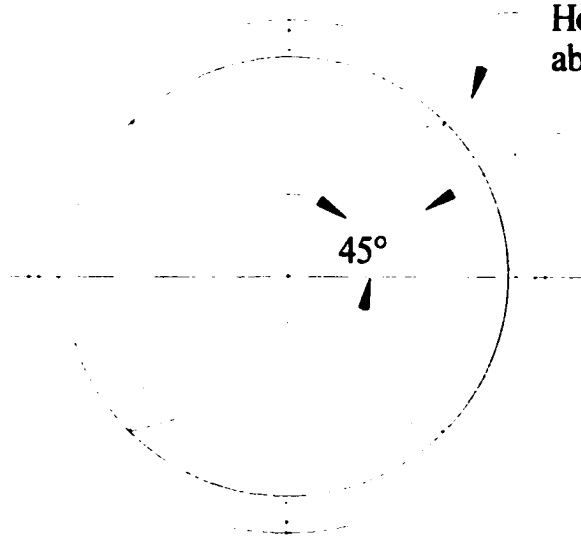

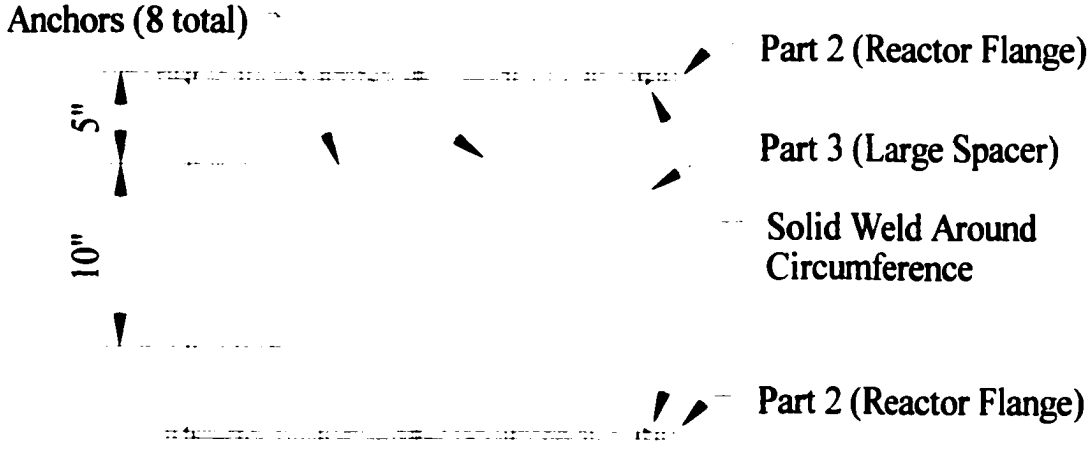

Assembled Small Spacer

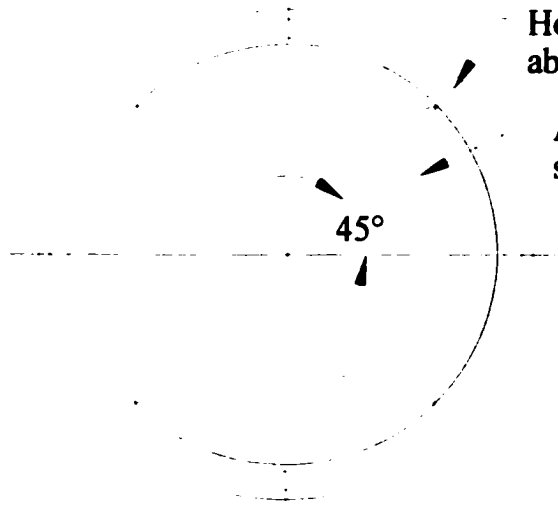

Holes in Flanges should line up above and below the small spacer

Anchors to be welded to inside surface of small spacer (4 total)

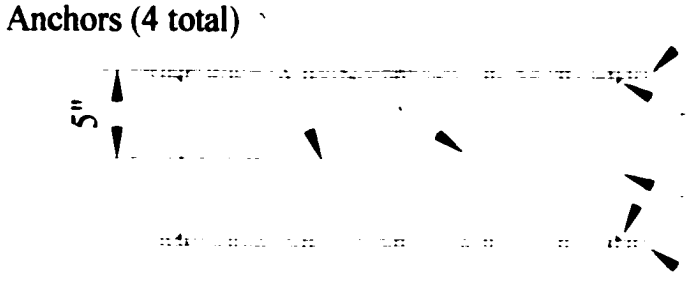

Assembled Sampling Zone

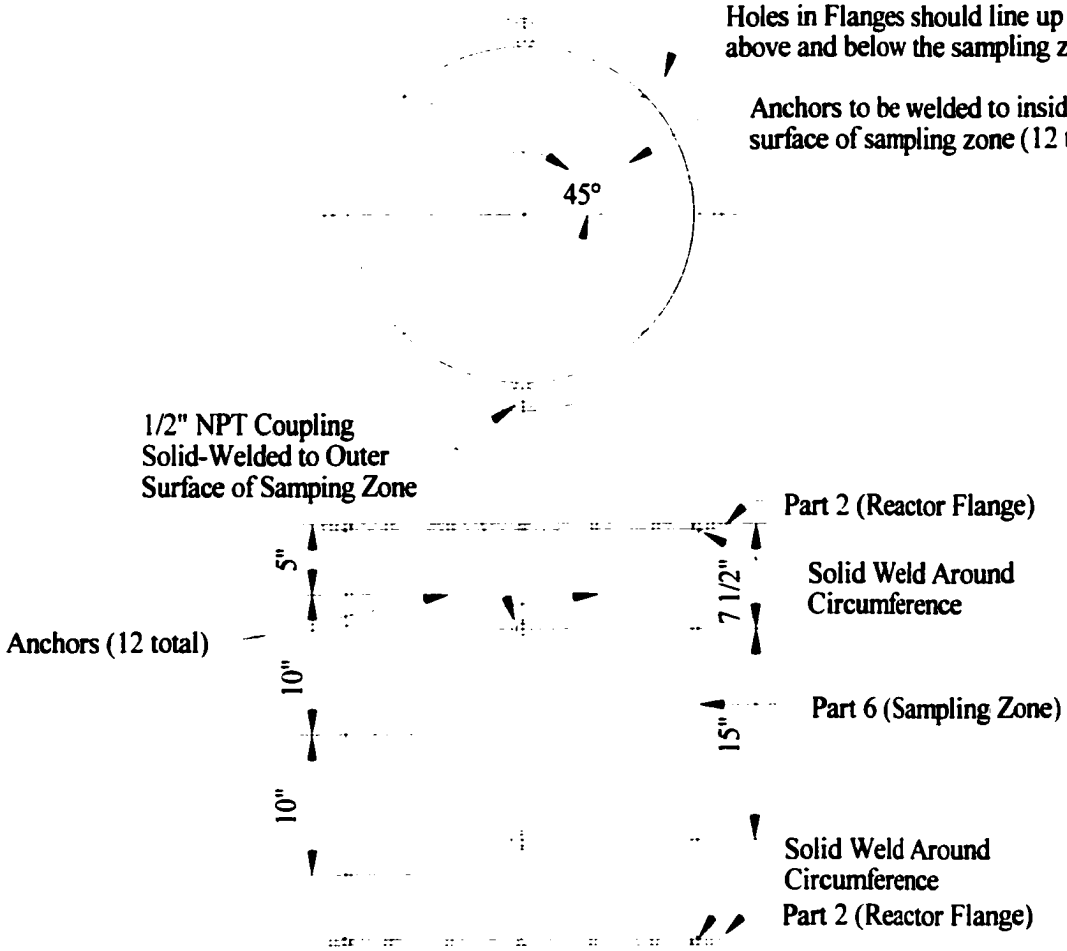

Assembled Bottom Section

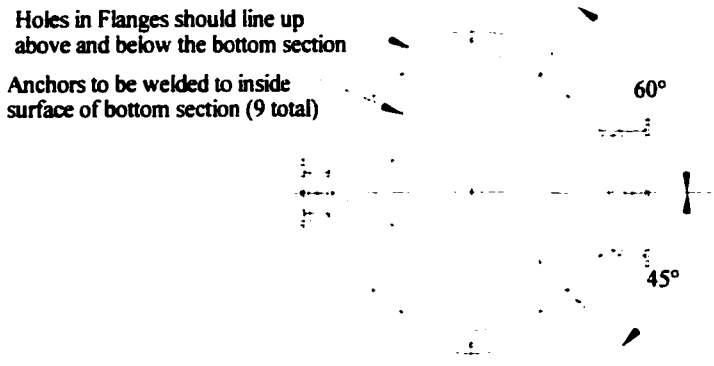

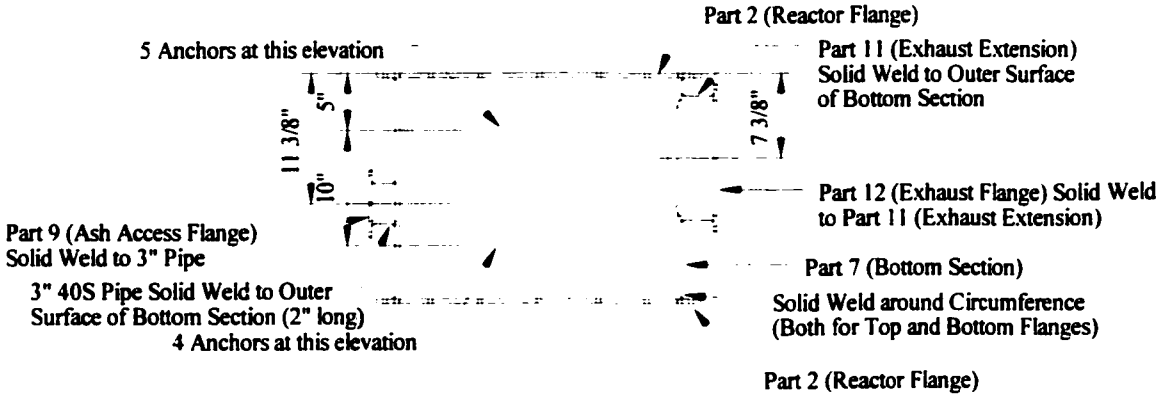

Assembled Feed Zone

1 1/4" 40S Nipple Solid Weld to
Outer Surface of Feed Zone (10" long)

Holes in Flanges should line up
above and below the feed zone

Anchors to be welded to inside
surface of feed zone (5 total)

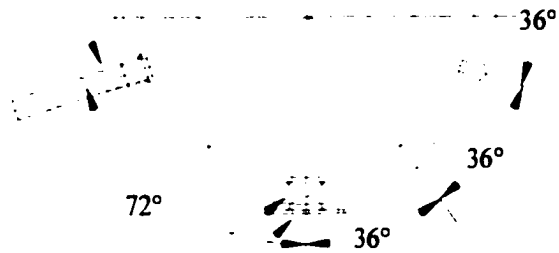

2" 40S Pipe Solid Weld to Outer
Surface of Feed Zone (2" long)

Part 13 (Feed Flange)
Solid Weld to Pipe

1/2" NPT Coupling Solid Weld to
Outer Surface of Feed Zone (2 total)

Part 2 (Reactor Flange)

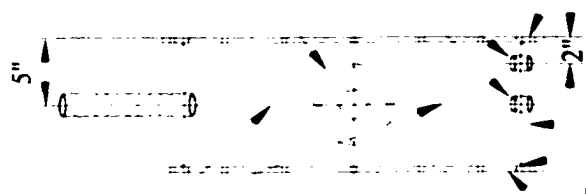

Part 4 (Feed Zone)
Solid Weld Around
Circumference

Anchors (5 total)

Part 2 (Reactor Flange)

APPENDIX B: BIOMASS HOPPER AND STEAM CALIBRATIONS

The rate that the biomasses used in this research were injected into the down-flow combustor were controlled by the variable-speed motor of the biomass hopper. The motor has settings from 1 – 8, indicating the relative speed of the metering auger. To calibrate the motor settings for each biomass, samples of biomass were collected for 5 minutes, then weighed, producing an empirical relationship between the speed of the metering auger and the flow rate of the injected biomass. Table 6 contains the raw data collected from these calibrations.

Table 6. Raw data for biomass calibrations.

Hopper Setting	g Alfalfa (10 min)	Alfalfa (g/min)	g Switchgrass (10 min)	Switchgrass (g/min)
1	66.2	6.62	49.6	4.96
2	142.6	14.26	86.4	8.64
3	215.8	21.58	129.0	12.90
4	275.3	27.53	165.1	16.51
5	315.8	31.58	206.1	20.61
6	378.8	37.88	224.4	22.44
7	434.6	43.46	272.6	27.26
8	459.7	45.97	295.8	29.58

The data were fitted with a second-order polynomial, forcing the intercept through zero, using Microsoft Excel trend-line functions. (14) is the polynomial expression for the alfalfa flow rate as a function of the biomass hopper setting, and (15) is the polynomial expression for the switchgrass flow rate as a function of the biomass hopper setting. Figure 37 is of the plotted data.

$$Alfalfa\ flowrate = -0.2356 \times setting^2 + 7.7079 \times setting,\ R^2 = 0.9971 \qquad (14)$$

$$Switchgrass\ flowrate = -0.1124 \times setting^2 + 4.5972 \times setting,\ R^2 = 0.9963 \qquad (15)$$

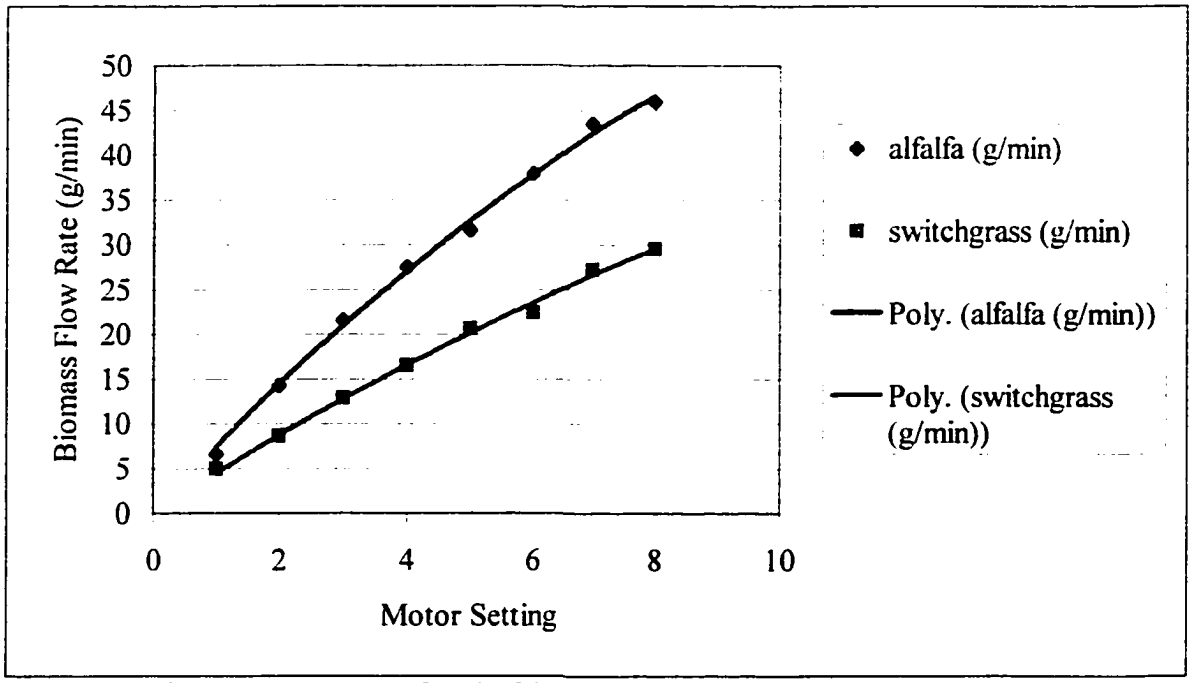

Figure 37. Calibration curves for the biomass hopper for alfalfa and switchgrass. Polynomial curves are second-order with y-intercept forced at 0.

To control the flow rate of steam used in this research, a precision metering needle valve was installed in the steam line, requiring 22 full turns of the valve before it is completely open. To calibrate this valve, a water-cooled condenser (Figure 38) was connected to the steam line. To calibrate a particular setting of the metering valve, sufficient water was fed to the water-cooled condenser to completely condense the steam flow rate, and the liquid condensate was weighed after collecting it for 10 minutes. Table 7 contains the raw data from this calibration experiment. Figure 39 is of the plotted data. The data was fitted with a second-order polynomial, forcing the intercept through zero, using Microsoft Excel trend line functions. Equation (16) is the polynomial expression for the steam flow rate as a function of the number of turns of the precision metering valve.

$$Steam\ flow rate = -0.844 \times (\#\ of\ turns)^2 + 24.95 \times (\#\ of\ turns),\ R^2 = 0.9944 \quad (16)$$

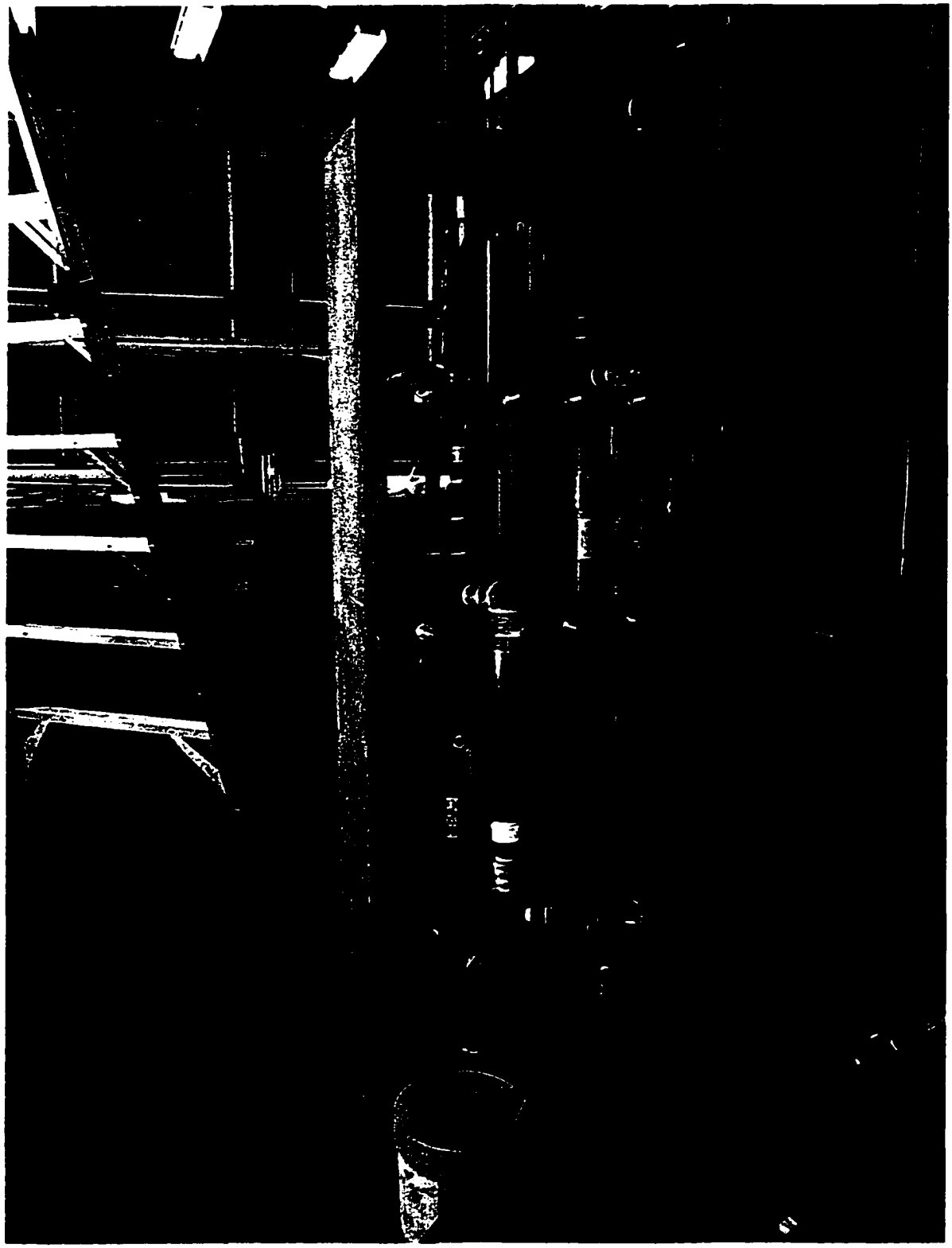

Figure 38. Water-cooled condenser used for steam calibration.

Table 7. Raw data from steam calibration.

# Turns of metering valve	g condensate (10 min)	Steam flow rate (g/min)
1	negligible	negligible
2	450	45
3	680	68
4	930	93
5	1070	107
6	1180	118
7	1330	133
8	1490	149
9	1510	151
10	1620	162
11	1740	174
12	1740	174
13	1790	179
14	1860	186
15	1880	188

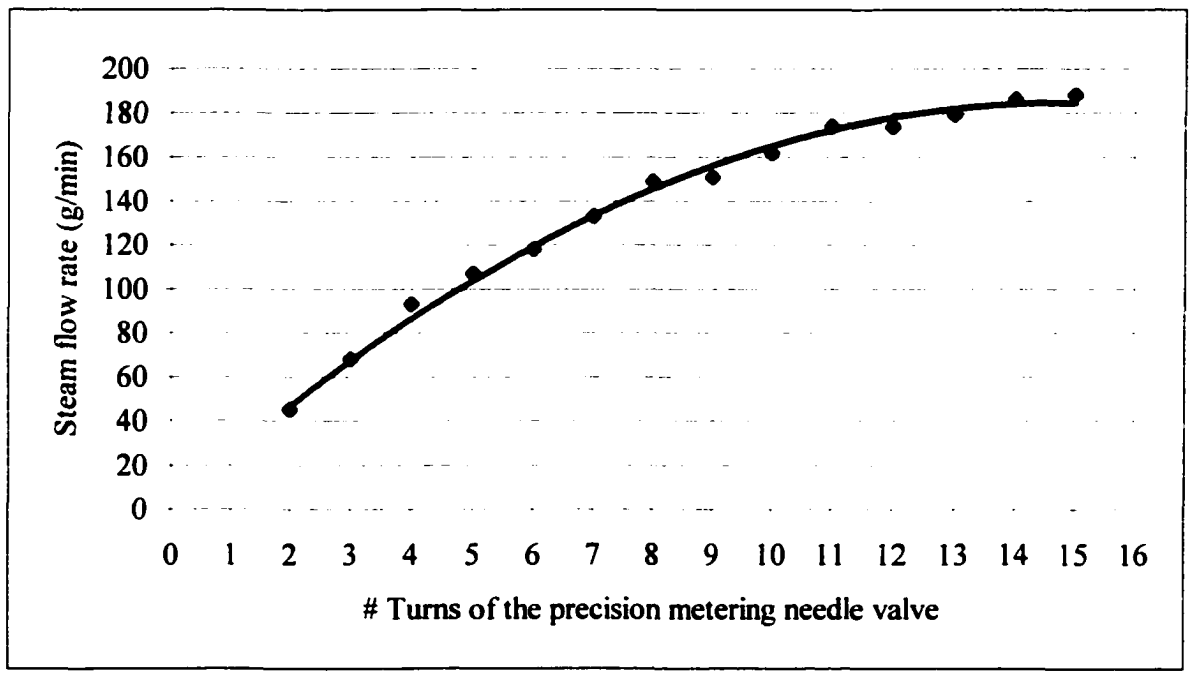

Figure 39. Steam flow rate calibration curve. Calibration curve is second order with y-intercept forced at 0.

APPENDIX C: COMPUTATIONAL FLUID DYNAMIC MODELING

SUMMARY REPORT

```
FLUENT
Version: 3d, segregated, spe2, ke (3d, segregated, 2 species, standard k-
epsilon)
Release: 5.5.14
Title:

Models
------

   Model                    Settings
   ---------------------------------------------------------
   Space                    3D
   Time                     Steady
   Viscous                  Standard k-epsilon turbulence model
   Wall Treatment           Standard Wall Functions
   Heat Transfer            Enabled
   Melting-Freezing         Disabled
   Radiation                None
   Species Transport        Non-Reacting (2 species)
   Coupled Dispersed Phase  Enabled
   Pollutants               Disabled
   Soot                     Disabled

Solver Controls
---------------

   Equations

      Equation     Solved
      -------------------
      Flow         yes
      Energy       yes
      Turbulence   yes
      o2           yes

   Numerics

      Numeric                          Enabled
      ---------------------------------------
      Absolute Velocity Formulation    yes

   Relaxation

      Variable                      Relaxation Factor
      ----------------------------------------------
      Pressure                      0.3
      Momentum                      0.7
      Energy                        1
      Turbulence Kinetic Energy     0.8
```

Turbulence Dissipation Rate	0.8
Viscosity	1
o2	1
Density	1
Body Forces	1
Discrete Phase Sources	0.5

Linear Solver

Variable	Solver Type	Termination Criterion	Residual Reduction Tolerance
Pressure	V-Cycle	0.1	
X-Momentum	Flexible	0.1	0.7
Y-Momentum	Flexible	0.1	0.7
Z-Momentum	Flexible	0.1	0.7
Energy	Flexible	0.1	0.7
Turbulence Kinetic Energy	Flexible	0.1	0.7
Turbulence Dissipation Rate	Flexible	0.1	0.7
o2	Flexible	0.1	0.7

Discretization Scheme

Variable	Scheme
Pressure	Standard
Momentum	First Order Upwind
Pressure-Velocity Coupling	SIMPLE
Energy	First Order Upwind
Turbulence Kinetic Energy	First Order Upwind
Turbulence Dissipation Rate	First Order Upwind
o2	First Order Upwind

Solution Limits

Quantity	Limit
Minimum Absolute Pressure	1
Maximum Absolute Pressure	5000000
Minimum Temperature	1
Maximum Temperature	5000
Minimum Turb. Kinetic Energy	1e-10
Maximum Turb. Viscosity Ratio	100000

Material Properties

Material: switchgrass (inert-particle)

Property	Units	Method	Value(s)
Density	kg/m3	constant	480
Cp (Specific Heat)	j/kg-k	constant	2310
Thermal Conductivity	w/m-k	constant	0.17299999

Material: mix (mixture)

Property	Units	Method	Value(s)
Mixture Species			
names	(o2 n2)		
Density	kg/m3	incompressible-ideal-gas	#f
Cp (Specific Heat)	j/kg-k	mixing-law	#f
Thermal Conductivity	w/m-k	mass-weighted-mixing-law	#f
Viscosity	kg/m-s	mass-weighted-mixing-law	#f
Mass Diffusivity	m2/s	constant-dilute-appx	(2.8799999e-05)
Thermal Expansion Coefficient	1/k	constant	0

Material: oxygen (fluid)

Property	Units	Method	Value(s)
Cp (Specific Heat)	j/kg-k	constant	919.31
Thermal Conductivity	w/m-k	constant	0.0246
Viscosity	kg/m-s	constant	1.919e-05
Molecular Weight	kg/kgmol	constant	31.9988
L-J Characteristic Length	angstrom	constant	3.458
L-J Energy Parameter	k	constant	107.4
Degrees of Freedom		constant	0

Material: water-vapor (fluid)

Property	Units	Method	Value(s)
Cp (Specific Heat)	j/kg-k	constant	2014
Thermal Conductivity	w/m-k	constant	0.0261
Viscosity	kg/m-s	constant	1.34e-05
Molecular Weight	kg/kgmol	constant	18.01534
L-J Characteristic Length	angstrom	constant	2.605
L-J Energy Parameter	k	constant	572.4
Degrees of Freedom		constant	0

Material: air (fluid)

Property	Units	Method	Value(s)
Cp (Specific Heat)	j/kg-k	constant	1006.43
Thermal Conductivity	w/m-k	constant	0.0242
Viscosity	kg/m-s	constant	1.7894001e-05
Molecular Weight	kg/kgmol	constant	28.966
L-J Characteristic Length	angstrom	constant	3.711
L-J Energy Parameter	k	constant	78.6
Degrees of Freedom		constant	0

Material: ceramic (solid)

Property	Units	Method	Value(s)
Density	kg/m3	constant	993
Cp (Specific Heat)	j/kg-k	polynomial	790 0.46250001
Thermal Conductivity	w/m-k	polynomial	0.25426 0.00020562

Material: silicon-carbide (solid)

Property	Units	Method	Value(s)
Density	kg/m3	constant	3160
Cp (Specific Heat)	j/kg-k	polynomial	289.42999 2.0472 -0.0015934 4.5509e-07
Thermal Conductivity	w/m-k	polynomial	196.92 -0.11237

Material: nitrogen (fluid)

Property	Units	Method	Value(s)
Cp (Specific Heat)	j/kg-k	constant	1040.67
Thermal Conductivity	w/m-k	constant	0.0242
Viscosity	kg/m-s	constant	1.663e-05
Molecular Weight	kg/kgmol	constant	28.013399
L-J Characteristic Length	angstrom	constant	3.621
L-J Energy Parameter	k	constant	97.53
Degrees of Freedom		constant	0

BIBLIOGRAPHY

1. Urich, J. Energy Systems Associates, Inc. Personal communication. January 7, 2002.
2. Schrecengost, R. A., B. P. Breen, A. F. Gomez, A. L. Huhmann, J. M. Pratapas, and R. A. Johnson. "Field Experience Testing Amine Enhanced Fuel Lean Gas Reburn At Public Service Electric & Gas Mercer Station." Presented at the 1998 Electric Power Research Institute NO_x Workshop. Baltimore, MD. August 24 – 26, 1998.
3. A look at U. S. air pollution laws and their amendments. Colby College. <http://www. colby.edu/sci.tech/cleanair/cleanairlegisl.htm> (Accessed April 10, 1999).
4. Prataps, J., and Bluestein, J. "Natural gas reburn: cost effective NO_x control." *Power Engineering*, Rice, A. L., ed. Tulsa, OK. 98(5), 47, 1994.
5. Clean Air Act Amendments of 1990. Office of Air and Radiation. United States Environmental Protection Agency. <http://www.epa.gov/oar/caa/caa101.txt> (Accessed April 10, 1999).
6. "Nitrogen oxides: impacts on public health and the environment." Office of Air and Radiation. United States Environmental Protection Agency. Washington, D.C. pp. 1 – 4. August 1997.
7. Energy Information Administration. "The effects of Title IV of the Clean Air Act Amendments of 1990 on electric utilities: an update." Office of Coal, Nuclear, Electric and Alternative Fuels, United States Department of Energy. Washington, DC. vii, March 1997.

8. "Summary Report – Control of NO_x emissions by reburning." Office of Research and Development, United States Environmental Protection Agency. Washington, D.C. pp. 3 – 18. February 1996.

9. Kokkinos, A. "Reburning for cyclone boiler retrofit NO_x control." *EPRI Jl.* 17, 36, 1992.

10. Combustion Technology: Some Modern Developments, Palmer, H. B., and Beer, J. M., eds. Academic Press. New York. 1974. pp. 18-19.

11. Glassman, I. Combustion, 2nd ed. Academic Press, Inc. Orlando, FL. 1987. p. 327.

12. Perry's Chemical Engineers' Handbook, 7th ed. McGraw-Hill, New York. 1997. p. 27-27.

13. Garg, A. "Specify better low-NO_x burners for furnaces." *Chem. Eng. Prog.* 90, 46, January 1994.

14. Wendt, J. O. L., Sternling, C. V., and Matovich, M. A. "Reduction of sulfur trioxide and nitrogen oxides by secondary fuel injection." In *Proceedings: Fourteenth Symposium (International) on Combustion.* The Combustion Institute, Pittsburgh, PA. August 1973. p. 897-904.

15. Chen, S. L., McCarthy, J. M., Clark, W. D., Heap, M. P., Seeker, W. R., and Pershing, D. W. "Bench and pilot scale process evaluation of reburning for in-furnace NO_x reduction." In *Proceedings: Twenty-First Symposium (International) on Combustion.* The Combustion Institute. Pittsburgh, PA. August 1986. p. 1159-1169.

16. Green, S. B., Chen, S. L., Pershing, D. W., Heap, M. P., and Seeker, W. R. "Bench scale process evaluation of reburning for in-furnace NO_x reduction." *J. Eng. Gas Turbines Power.* 107(3), 450, 1986.

17. Kilpinen, P., Glaborg, P., and Hupa, M. "Reburning chemistry: a kinetic modeling study." *Ind. Eng. Che. Res.* 31(6), 1477, 1992.

18. Bilbao, R., Millera, A., and Alzueta, M. U. "Influence of the temperature and oxygen concentration on NO_x reduction in the natural gas reburning process." *Ind. Eng. Chem. Res.* 33(11), 2846, 1994.

19. Brouwer, J., Heap, M. P., Bales, F. E., Inkley, D. S., Lighty, J. S., and Pershing, D. W. "The use of wood as a reburning fuel in combustion system." In *Proceedings: Bioenergy `94, 6th National Bioenergy Conference*, Farrell, J. Sargent, S., Swanson, D., and Nelson, R., eds. Western Regional Biomass Energy Program, Lincoln, NE. October 1994.

20. Bilbao, R., Alzueta, M. U., and Millera, A. "Experimental study of the influence of the operating variables on natural gas reburning efficiency." *Ind. Eng. Chem. Res.* 34(12), 4531, 1995.

21. Zamansky, V. M., Maly, P. M., Seeker, W. R., and Folsom, B. A. "Biomass fuels in reburning technologies." In *Proceedings: Biomass for Energy and Industry, 10th European Conference and Technology Exhibition.* June 1998.

22. Liu, H., Hampartsoumian, E., and Gibbs, B. M. "Evaluation of the optimal fuel characteristics for efficient NO reduction by coal reburning." *Fuel.* 76(11), 985, 1997.

23. Miller, C. A., Lemieux, P. M., and Touati, A. "Evaluation of tire-derived fuel for use in nitrogen oxide reduction by reburning." *J. Air and Waste Management Assoc.* 48(11), 729-735, 1998.

24. Harding, N. S., and Adams, B. R. "Biomass as a reburning fuel: a specialized cofiring application." *Biomass Bioenergy.* 19, 429-445, 2000.

25. Bilbao, R., Alzueta, M. U., Millera, A., and Duarte, M. "Simplified kinetic model of the chemistry in the reburning zone using natural gas." *Ind. Eng. Chem. Res.* 34(12), 4531-4539, 1995.

26. Fluent, Inc. Lebanon, NH.

27. Jones, W. P., and Launder, B. E. "The prediction of laminarization with a two-equation model of turbulence." *Intl. J. Heat Mass Trans.* 15(2), 301-314, 1972.

28. Breen, Bernard. Energy Systems Associates, Inc. Personal communication. February 1, 2002.